Reply to the reviewers.

Review 1:

Review of *"Influence of vessel characteristics and atmospheric processes on the gas and particle phase of ship emission plumes: In–situ measurements in the Mediterranean Sea and around the Arabian Peninsula"* by Celik et al, submitted to ACPD.

In their manuscript, the authors present data and analysis of measurements of over 250 ship emission plumes in the Mediterranean and around the Arabian Peninsula. From the data, the authors present information on the dispersion of the ship plumes, as well as comprehensive data on different components of the emission plumes. The manuscript also connects these observations to ship characteristics obtained from the AIS system. Finally, the authors also discuss the different atmospheric processes that affect the various components of the plume.
The manuscript's topic is very well suited to Atmospheric Chemistry and Physics, and the data and its analysis are interesting and of potentially high value. The paper is well structured and easy to read. Therefore, in principle the paper should be considered for publication in ACP. However, I think there are a few mistakes in the methodology and the reasoning behind drawing some conclusions, especially with a) the interpretation of the black carbon (BC) data and b) the computation of the O:C ratios. These are significant enough that they must be corrected before the paper is published in ACP, as they might change some of the presented results.

Reply: We thank the reviewer for this very positive general comment on our manuscript.

In the following, I will first discuss these two possible issues, and then give other general comments on the manuscript:

1. BC data dependence on pressure and temperature
I have serious reservations regarding the conclusion driven from the BC data dependence on ambient temperature and pressure (if I understood correctly). To my understanding, the ambient temperature and pressure only affect the gas concentration (in units of molecules/m$_3$) and don't affect the fraction of oxygen in a given mass of air. As in a diesel engine the air is in any case highly compressed, the amount of oxygen available should not change too much. There certainly is the possibility that there might be other pressure/temperature effects that affect engine operation, but to use p/T as a proxy for these, the effects should be more thoroughly explained and appropriate references given.

Additionally, I see a potential alternative explanation to the observation: I'm not fully aware on how the flow calibration for the BC instrument has been performed. However, If the instrument pump pushes a constant mass (or constant number of molecules) per unit time through the filter, i.e. n = pV/kT = constant (as would be the case with a mass flow controller), then as the value of p/T increases, the volume going through the filter decreases. As the derived BC concentration depends in a non-linear way (as explained in Drinovec et al., 2015, which the authors also cite) from the change in attenuation and also the volume flow rate, I think it is conceivable that the observation in Fig 3 is caused by this effect. This should be considered seriously, especially with the reported periodicity of the instrument reading with respect to the measurement container temperature control.

I would suggest reviewing and re-analysing the BC data and its conclusions. For example, it would be informative to see if the BC concentration vs. p/T -dependence is visible only for plumes, or also for ambient BC concentration measurements.

Reply: Thank you very much for this very important comment. As a consequence of this comment we thoroughly reviewed the BC data. According to the manufacturer of the Aethalometer, which was used to determine BC concentrations, the instrument uses a mass flow controller to regulate the flow through the instrument. However, such effects as described by the reviewer should still not occur, because in this instrument the pressure and temperature of the flow are also monitored and the measurement results are internally converted to standard conditions.
Unfortunately, the BC concentrations vs. p/T-dependence of ambient BC concentration measurements cannot be assessed, since in ambient measurements BC concentrations depend strongly on the air mass history.

In order to assess this issue further we have determined whether we can also find a p/T dependency of the NOx emission factor, which is also known to have a dependency on combustion efficiency. In agreement with our findings for BC we found an increase in EF_{NOx} *with increasing p/T, i.e. also suggesting increasing combustion efficiency with increasing p/T. We find it very unlikely that both of these independent instruments generate inverted trends (BC decreases, NOx increases) as a consequence of p/T changes.*

In a further step we have searched the literature for information on internal combustion engine performance dependency on ambient air conditions. According to the literature a decrease in ambient pressure and an increase in ambient temperature can result in reduced engine performance, in agreement with our findings (Bermudez et al., 2017; Chang et al., 2017; Rajewski, 2018). Furthermore, ambient humidity is also known to deteriorate combustion efficiency, resulting in reduced NOx and increased soot emissions. In agreement with this, we also found a general increase in our BC emission factors and a decrease in our NOx emission factors with increasing ambient (absolute) humidity. The use of turbochargers and intercoolers in marine diesel engines reduces the influence of ambient conditions onto the combustion process, but apparently does not completely suppress it. This is also in accordance with information from the literature (Chang et al., 2017).

As a consequence of these findings we slightly extended the respective statement and added the correlation plots for BC on H2O concentration as well as for NOx on p/T and H2O concentration to the manuscript (see revised Fig. 3). The statement in the main text now reads:

"… In general, more efficient fuel combustion results in increased NO_x (especially NO) emissions owing to the enhanced oxidation of atmospheric nitrogen that occurs at higher combustion temperatures. It also leads to decreased soot particle (*here*: BC) emissions as a consequence of more efficient oxidation of fuel carbon (Corbett et al., 1999; Juwono et al., 2013; Pokhrel and Lee, 2015). The fuel combustion efficiency depends primarily on the oxygen–to–fuel mixing ratio in the combustion chamber (Khalid, 2013), but also increased ambient temperature and absolute humidity as well as reduced ambient pressure can result in deteriorated combustion efficiencies of diesel engines, associated with elevated soot and reduced NO_x emissions (Bermudez et al., 2017; Chang et al., 2017; Rajewski, 2018). Even though the use of turbochargers and intercoolers in marine diesel engines should minimize the influence of ambient conditions onto the combustion process, we found indications for combustion efficiency dependence on such variables. With increasing ambient pressure *p* and decreasing temperature *T*, as well as for an increase in the p/T ratio (Fig. 3(a)), a reduction of the BC emission factor by more than a factor of 2 over the range of observations and a general increase of the NO_x emission factor were observed, both indications for improved combustion efficiency (see below). Likewise, deteriorated combustion efficiency with increasing ambient absolute humidity is suggested by the observed dependencies of the BC and NO_x emission factors on ambient water vapor concentration (Fig. 3(b)). "

2. Calculation of O:C ratios

I had some trouble following the definitions in eqs 3-5; I think there's an error in the definition of the terms. Assuming that O/C and H/C ratios refer to the atomic ratios, the second version for the computation of the concentration of [O] and [C] are wrong. This can be illustrated with an example: an organic compound with 5 oxygens, 3 hydrogens, and 3 carbons, so we get the following values

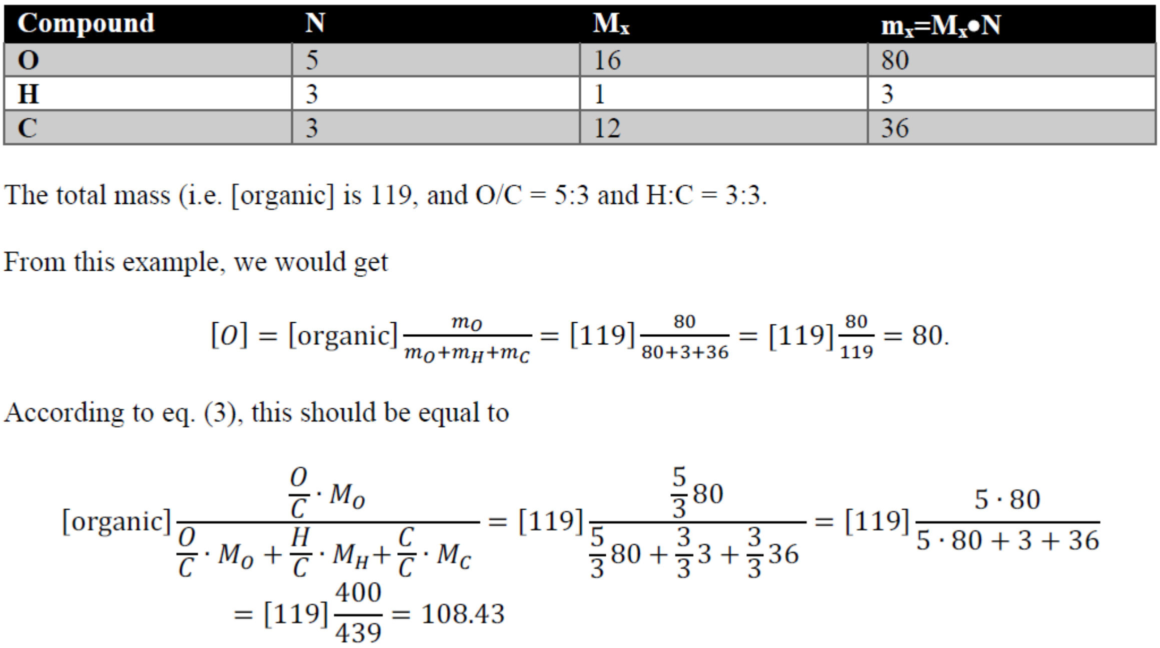

Compound	N	M_x	$m_x=M_x \bullet N$
O	5	16	80
H	3	1	3
C	3	12	36

The total mass (i.e. [organic] is 119, and O/C = 5:3 and H:C = 3:3.

From this example, we would get

$$[O] = [\text{organic}]\frac{m_O}{m_O+m_H+m_C} = [119]\frac{80}{80+3+36} = [119]\frac{80}{119} = 80.$$

According to eq. (3), this should be equal to

$$[\text{organic}]\frac{\frac{O}{C}\cdot M_O}{\frac{O}{C}\cdot M_O+\frac{H}{C}\cdot M_H+\frac{C}{C}\cdot M_C} = [119]\frac{\frac{5}{3}80}{\frac{5}{3}80+\frac{3}{3}3+\frac{3}{3}36} = [119]\frac{5\cdot 80}{5\cdot 80+3+36}$$
$$= [119]\frac{400}{439} = 108.43$$

which gives an error of 35% compared to the first equation for [O].

Reply: We have checked the formula once again and did not find an error with it. In the calculation presented by the reviewer, however, we found an error:

Using the values from the table provided by the reviewer (C3H3O5 as example substance) in the formula for [O] we get, largely in agreement with the calculation by the reviewer

$$[O] = \ [organic]\frac{m_O}{m_O+\ m_H+\ m_C} = [organic]\frac{80}{80+3+36} = [organic]*\frac{80}{119}$$

Note, that [organic] is the actually measured total particulate organics mass concentration, determined by the AMS. It is not the molecular weight of an individual molecule. In the revised version of the manuscript we stress this further.

According to equation (3) this should be equal to

$$[organic]\,\frac{\frac{O}{C}\,M_O}{\frac{O}{C}\,M_O+\frac{H}{C}\,M_H+\frac{C}{C}\,M_C}=[organic]\,\frac{\frac{5}{3}\,16}{\frac{5}{3}\,16+\frac{3}{3}\,1+\frac{3}{3}\,12}$$

$$=\ [organic]\frac{80}{80+3+36}\ =\ [organic]*\frac{80}{119}$$

The difference (besides the fact that for [organic] no value was introduced, which however does not make a difference in the overall calculation) is that for M_O, M_H, and M_C the atomic weights of O, H, and C need to be used (as stated in the manuscript text and in the table above) and not their atomic weights multiplied by the number of atoms in the molecule. Then the result of both formulae is the same as presented above.

To avoid confusion, we therefore slightly extended the text around the formula to make this clearer:

*"*Using the measured mass concentrations of particulate organics ([organics]) and the atomic O/C and H/C ratios for the organic aerosol during plume and background measurements, the O/C ratios for the plume contribution were calculated (Eq. 6) from the average mass concentrations of oxygen and carbon for both the background (B) and for the ship emission event (emission + background, EB). The mass concentrations of O and C were calculated from the mass fraction of oxygen and carbon in the organic aerosol, determined from the measured atomic O/C and H/C ratios, following Eqs. (4) and (5):

$$[\mathbf{O}]=\frac{[\mathbf{organics}]\cdot \boldsymbol{m}_{\mathbf{O}}}{\boldsymbol{m}_{\mathbf{O}}+\boldsymbol{m}_{\mathbf{H}}+\boldsymbol{m}_{\mathbf{C}}}=\frac{[\mathbf{organics}]\cdot\mathbf{O/C}\cdot\boldsymbol{M}_{\mathbf{O}}}{\mathbf{O/C}\cdot\boldsymbol{M}_{\mathbf{O}}+\mathbf{H/C}\cdot\boldsymbol{M}_{\mathbf{H}}+\mathbf{C/C}\cdot\boldsymbol{M}_{\mathbf{C}}},\qquad(4)$$

$$[\mathbf{C}]=\frac{[\boldsymbol{organics}]\cdot \boldsymbol{m}_{\boldsymbol{C}}}{\boldsymbol{m}_{\boldsymbol{O}}+\boldsymbol{m}_{\boldsymbol{H}}+\boldsymbol{m}_{\boldsymbol{C}}}=\frac{[\mathbf{organics}]\cdot\boldsymbol{M}_{\mathbf{C}}}{\mathbf{O/C}\cdot\boldsymbol{M}_{\mathbf{O}}+\mathbf{H/C}\cdot\boldsymbol{M}_{\mathbf{H}}+\boldsymbol{M}_{\mathbf{C}}},\qquad(5)$$

$$\mathbf{O/C}=\frac{([\mathbf{O}]_{\mathbf{EB}}-[\mathbf{O}]_{\mathbf{B}})/\mathbf{M}_{\mathbf{O}}}{([\mathbf{C}]_{\mathbf{EB}}-[\mathbf{C}]_{\mathbf{B}})/\mathbf{M}_{\mathbf{C}}},\qquad(6)$$

where m_x is the (measured) total mass and M_x the atomic weight of the respective species x. For these calculations we assume that particulate organics consist only of oxygen, hydrogen and carbon. To check for consistency, the H/C ratio was calculated analogously and found to always show the expected reverse behaviour to the O/C ratio."

For these calculations, it is also unclear, which of the equations was used for the actual computation of the values. This should be clarified, and in case it has an effect on the results, the new results presented in the revised manuscript.

Reply: As discussed above, both equations are equal. The second equation was used to calculate [O] and [C]. To make this clearer we also added some text to this equation as shown above.

3. General Comments

- Pg.2, line 1: “The results enable identification of…”: I think the identification has already been done, so this should be reflected here.

*Reply: Thank you for this comment. The sentence was not clear enough and could be misunderstood. Therefore, we changed it to: “*The results allow to describe the influences on (or processes in) ship emission plumes quantitatively by parameterizations, which could be used for further refinement of atmospheric models, and to identify which of these processes are the most important ones.*”*

- Pg 4, line 14: “…appropriate inlet systems”: The sampling lines can have profound effects on the measured quantities, so I think it would be good to elaborate a little on the sampling line system. If some known guidelines for the sampling were followed, a reference could be given. Are the losses given in Table 1 the line losses? If yes, were they calculated or experimentally determined?

Reply: Within this study, measurements from 11 different instruments were used, which utilized a variety of different inlet lines, each optimized for the respective measurement. For the aerosol instruments a common inlet system was used. Particle losses within this inlet system were estimated using the Particle Loss Calculator (von der Weiden, et al., 2009) as mentioned in the main text. We now added this information also to the caption of Table 1 and also made clearer that these losses are transport losses. To avoid a lengthy discussion on the various inlet systems of all instruments we need to refer to the respective publications where the various data sets are presented by the operators of the instruments for more details.

- Page 5, line 15: I think it could be good to clarify the PM1 calculation algorithm: I think based on the explanation it is PM1 = V_{FMPS} * r_{AMS+BC}*F_{corr}
where V_{FMPS} is the volume obtained from FMPS, r_{AMS+BC} is the average density obtained from AMS and BC measurements, and F_{corr} is a correction factor that mostly accounts for underestimated concentrations >130 nm. As the correction factors are averages estimated from the data, I think it would be good to give some information on the variation, eg. Give the standard deviation of r_{AMS+BC} and F_{corr}. Also, if the OPC was measuring large particles, should it be included in Table 1?

Reply: Thank you for this suggestion. To improve clarity of the PM1 calculation procedure we included the suggested formula into the text and added the other requested information:
*“*As the ship emission plumes measured during the AQABA field campaign showed particles exclusively in the (lower) size range of the FMPS, this data was used to calculate PM_1 particle mass concentrations from the FMPS-derived total particle volume concentration (V_{FMPS}), assuming spherical particles and an average particle density of 1.53 g cm^{-3} calculated using the mass concentrations of AMS species and BC (ρ_{AMS+BC}). The calculated PM_1 particle mass concentrations were corrected for under–measurement in the upper size range of the FMPS (> 130 nm; Levin et al., 2015) by scaling them with a factor of F_{corr}=1.85, which was derived from comparison with size distribution data from a concurrently measuring Optical Particle Counter (OPC, Grimm Model 1.109):

$$PM_1 = V_{FMPS} \cdot \rho_{AMS+BC} \cdot F_{corr} \quad . \tag{1}$$

While V_{FMPS} are actually measured data for each plume event, F_{corr} and ρ_{AMS+BC} are the average correction factor for the under-measurement in the upper FMPS channels and the average particle density, determined from AMS and BC measurements for the whole field campaign. The overall uncertainty of the resulting PM_1 concentrations is estimated to be 35%."

As mentioned in the manuscript, no large particles (larger than the size range covered by the FMPS) were found in the ship emission plumes. Therefore, the OPC data were not used to derive information on the ship emissions. The OPC data from the out-of-plume measurements were only used to correct the upper size range of the FMPS for under-measurement as mentioned in the text. Because the OPC data are not included in the presented analysis, we feel that this instrument should not be included in Table 1, as well as many other instruments which were operated on-board the research vessel and which were also not used for this analysis.

- Page 5, line 31: "..linear or Gaussian fits." Here it is unclear what was fitted to what. Could this be elaborated?

Reply: We re-worded the corresponding sentences to make clearer what we have done:
"Some of the gas phase data, especially those of the nitrogen oxides, show periodic gaps of 1 to 2 min duration due to periodic background measurements or calibrations. These affected in some cases the detected ship emission events. If possible, the affected events were reconstructed using the remaining parts of the times series by either linear or Gaussian fits, depending on the expected shape of the missing part of the peak."

- Page 8, line 11: "..linearly interpolated": I think this is just taking the mean background from before and after the plume. Is this so?

Reply: This is correct. We re-worded this sentence to make this clear:
"The mean background was calculated from the average values derived for the two background intervals and subtracted from the average event concentration to obtain the average excess concentration in the plume."

- Line 14-15: "defined as …": it would be easier to read this just as a formula I think.

Reply: We agree with the reviewer and expressed the definition of the detection limit as formula:
"In general, calculated average excess concentrations below the detection limit ($LOD = \frac{3\,\sigma_{bg}}{\sqrt{n}}$, with σ_{bg} the standard deviation of the background and *n* the number of measurement points within the ship emission event interval) were excluded from further analysis."

- Page 9, line 4: “dispersion time constant”: As there are several ways of defining time constants, I think it is important to say which one is meant. Is it the concentration half-life, or e-folding time, or some other one?

Reply: As dispersion time constant we use the e-folding time. We added this information to the text.

- Page 9, line 13: “one standard deviation”: I think this should be geometric standard deviation

Reply: Thank you. We added this to the text.

- Page 9, line 20: “measured OH concentrations were not used… only describe the situation and the research vessel’s position and not within the plume”. Is this not also the case for the photolysis rate?

Reply: The photolysis rate JO^{1}D *is determined from the spectrally resolved irradiation. Only under special conditions, e.g. when there are strong spatial gradients in cloud coverage, this variable is strongly different along the path from the emission position to the measurement position. Generally, we assume that it is a much more robust variable compared to the locally measured OH concentration, which is affected by a multitude of influences. Therefore, we assume that normally this variable is a good proxy for potential photochemical processing during the plume transport. To make this point clearer we changed the sentence to:*
*“*Measured OH concentrations were not used as a measure of photochemical processing due to insufficient data coverage and because they are more affected by local influences than the photolysis rate and therefore more so than the latter describe merely the situation at the research vessel’s position rather than within the plume.*”*

- Page 12, line 5-10: A reduction of particle number EF was observed with vessel size, and this is attributed to coagulation. Is this the only explanation, or could there be others too? What is the variation in the residence time?

Reply: Of course, there are many potential reasons why particle number emission factors could vary. This includes (unknown) details about the design of the burning chambers, the burning conditions or other factors which affect the generation of particulate emissions. Typically, an important factor influencing particle number concentrations is coagulation at high particle number concentrations. Since we expect longer residence times in the exhaust system of larger ships, it makes sense to assume a stronger influence of coagulation on particle number concentration in such ships. Since we state that our observation is “in agreement with this”, we do not claim that this is the one and only explanation for our observation. We do not know the residence time of the exhaust in the individual ships and therefore we also do not know the variation of residence times. We therefore clarified this in this sentence:
*“*Longer residence times within the exhaust system, as they typically occur in larger ships, should therefore result in lower particle number concentrations due to enhanced coagulation effects.*”*

- Page 12, line 12, and pg 19, line 7. -> I find the finding on the wind speed influencing the effective EF interesting. I think this is an important effect to take into consideration. However, I think that it should be made clear that at the source, the emission is the same – the difference in the observed EF is introduced only later during the processing of the plume. Additionally, I'd like to know the more detailed reasoning behind this, as to me, the increased dilution in at high WS should be accounted for in the calculation. Is the age of the plume (since emission) factored in here? Does the wind speed affect engine operation?

Reply: As written within the text, we treat the initial dilution of the exhaust from the stack of the ship into the atmosphere as part of the emission process. However, we agree with the reviewer that we should make the influences of the different parts of this emission process clearer. Therefore, we changed the sentence to:
*"*However, even for a given particle number concentration at the location of emission, the level of further coagulation depends on the concentration level in the transported plume, which is expected to depend on the ambient wind speed, as it influences the degree of dilution in this phase of emission.*"*
Since we do not discuss absolute concentrations but emission factors (i.e. concentrations normalized to defined amounts of fuel), the effects of dilution (both, due to different wind speed as well as due to different transport times) are already accounted for in the EFs. Therefore, if we find an influence of wind speed onto particle number concentration EFs, this should reflect a real influence of wind speed onto particle number concentrations in the emission plumes.
Because on average ships do not travel in a certain direction with respect to wind direction (e.g. preferentially in opposite direction as the wind direction), we do not expect a general influence of wind speed on engine operation.

- With regard to the wind speed, was there a correlation with the plume dispersion time constant (page 9) and wind speed? As the explanation for the effect on particles is related to dilution, I think there might be a connection between the two. If not, why?

Reply: This is an interesting point. Unfortunately, due to the many factors influencing the various emission factors, concentrations and other variables, it was not possible to determine e.g. dispersion time constants separately for different wind speed conditions. Therefore, we unfortunately cannot answer this question.

- More generally, I think that the term emission factor (EF) should be used only for actual emission at the point and time of emission, and if the observed aerosol after some time has some differing characteristics, this should be noted with some qualifier, e.g. 'apparent' or 'effective'.

Reply: Thank you, this is a very good point. We revised the usage throughout the text and use the term "emission factor" only for those EF which were either determined for the point of emission or do not change over transport time, and use the term "apparent emission factor" for those EF which were altered during processes occurring during transport. We introduce *the term "apparent emission factor" in Sect. 2.4, where the general emission factor calculation is presented (page 9).*

- Figure 2: I have some trouble understanding the decision-making when two ships are in the path of an air mass. In the example given, it seems to me from the figure that both the red and the blue ship are relevant for the observed plume. Why was the blue ship not considered? This could be clarified.

Reply: The position of the ships at the time when the back-traced air mass intersects the reconstructed ship track is indicated by the "ship" label (see legend of Figure 2). For the red ship this position is within the wind direction sector, while for the blue ship it is outside this sector. Therefore, at the time when the air mass intersected the ship track, the red ship was at the intersection point while the blue one was not.
To make this clearer we re-worded the figure caption:
"Two AIS records (position indicated by dots on the vessel tracks) were requested after the AQABA field campaign from the AIS data base for each of these vessels … The uncertainties of the intersection times and of the corresponding vessel positions (ship markers on the vessel tracks) are based on the uncertainties of the wind speed."

References:

Bermudez, V., Serrano, J. R., Piqueras, P., Gomez, J., Bender, S.: Analysis of the role of altitude on diesel engine performance and emissions using an atmosphere simulator, International Journal of Engine Research 18, 105-117, DOI:10.1177/1468087416679569, 2017.

Chang, Y., Mendrea, B., Sterniak, J., Bohac, S. V.: Effect of Ambient Temperature and Humidity on Combustion and Emissions of a Spark-Assisted Compression Ignition Engine, J. Eng. Gas Turbines Power, 139, 51501-1 – 51501-7, https://doi.org/10.1115/1.4034966, 2017.

Rajewski, A.: Evaluating internal combustion engine's performance, Wärtsilä Technical Journal 2/2018, 18-23, 2018.

Review 2:

Interactive comment on "Influence of vessel characteristics and atmospheric processes on the gas and particle phase of ship emission plumes: In-situ measurements in the Mediterranean Sea and around the Arabian Peninsula" by Siddika Celik et al.

Mingxi Yang (Referee)

This paper presents an analysis of a large dataset of ship plumes measured from a research vessel in the Mediterranean. It's a very impressive data set with many gas and particle phase instruments. The

authors used AIS ship positioning to attribute measured ship plumes to individual ships, a non-trivial exercise.
The various emission factors were computed (accounting for plume dilution) and then related to ship/engine characteristics, operational conditions, atmospheric conditions, etc. The paper is generally well written and the data will be very useful for better understanding of ship emissions.

Reply: We thank the reviewer for this very positive overall comment on our manuscript.

Because a large number of ships were measured, and because it's not possible to follow individual ship plumes in a Lagrangian fashion from a research vessel, the analysis is generally done on all the detected plumes as a whole, with a lot of bin-averaging involved. This unfortunately buries many details and real sources of variability. I would like to see the authors trying to tease out some of those complexities (see detailed comments below). I think the authors should make it clear at the beginning that their measurements are not Lagrangian (i.e. following the same ship plume over time). Thus, their observations of the effect of plume aging represent the variability of an ensemble of initially different plumes at various stages of aging. The observations don't uniquely capture the plume aging effect and this should be acknowledged.

Reply: Thank you for this important comment. We realize that we did not make sufficiently clear that our analysis approach is not based on Lagrangian measurements of individual plumes but on the measurement of plume ensembles and deduction of dependencies on various variables from such ensembles. We revised the paragraph where such general remarks on our analysis approach are introduced (beginning of Sect. 3; see below) to make this clearer.

The reviewer is right, bin-averaging does bury much of the variation within the measurement data. On the other hand, it provides a clearer picture to the reader about potential dependencies of emission factors on certain external variables. To make use of both, the whole information within the un-binned data and the improved clarity of the binned emission factors, we used the former ones to calculate the correlations and parameterizations provided in Table 2 and the latter ones to generate most of the Figures. To make this clearer, we revised the respective text in the manuscript (Sect. 3; see below).

We completely agree with the reviewer that within the variability of the un-binned data a lot of information about additional dependencies of emission factors on other external parameters is buried. In our analysis of the data we tried to tease out this information with three different methods, (1) color-coding the markers in the correlation plots depending on the magnitude of a third variable, (2) producing separate correlation plots for sub-sets of the emission factors, and (3) correlating the emissions factors with several potentially influencing factors in separate correlation plots. Because most of the emission factors depend on multiple (and not only one or two) external parameters and because the number of data points in each of such plots is very limited (i.e. to the number of available data points, i.e. plumes, for which all variables of interest are available at the same time), the first two of these approaches did not result in conclusive additional information for most of the emission factors. Only for a few of the correlations significant differences were found (and are already presented in the manuscript), e.g. in some cases when differentiating between day and night measurements, as for example done for the particle number emission factor (Figure 9c). For most of the emission factors where differences between night and day were found, it was more conclusive to use photochemical plume age as independent variable in the correlation plots, which already includes this effect (day/night). For individual emission factors mentioned in the detailed comments below we provide the respective correlation plots with separated correlations for day and night either in this reply or in the supplementary material (see replies to comments below). In addition, we add this information about the reason why no additional secondary dependencies of emission factors could be teased out and therefore are not presented in the revised manuscript (Sect. 3):

“Parallel measurements of multiple variables which are associated with ship emission plumes and observation of such plumes under very different conditions (e.g. plume age, meteorological conditions, source vessel characteristics, etc.) allow the investigation of factors which might influence the characteristics of ship emission plumes. For this purpose, we investigated the relationship between plume characteristics and various factors (above mentioned measurement conditions) by correlation analysis, which, contrary to Lagrangian measurements of individual ship plumes during transport away from the source, provide ensemble-averaged information on emission or transformation characteristics of plume properties. As several different factors can influence individual plume characteristics, the correlation plots always show a relatively strong degree of scatter, which led us to bin them, such that the same number of data points (at least 5 and maximal 32) was included in each bin, resulting in not equidistantly distributed bins. The slope and intercept did not significantly change when using binned data instead of raw data. Therefore, fit parameters for the correlation of raw data are presented in Table 2, while in the figures usually the binned data are shown for clarity. In case raw data are presented their relative uncertainties combine the estimated quantification (Sect. 2.4) and measurement uncertainties, whereas in case of binned data error bars include in addition one sigma standard deviations of the data distributions in each bin. Using bin-averaged data or linear regressions strongly reduces the influence of additional influencing factors on the individual data points and, to a large degree, provides information on the dependence of the respective plume feature on the influencing factor under investigation. To extract the influence of several influencing external factors on plume characteristics, separate correlation plots for each of these factors were therefore generated.”

The different emission factors as a function of plume age/photochemical processing is very interesting. Can author say something about the max distance (or time) down wind of source for which the various EF estimates still represent stack emissions?

Reply: This is a very good point. Indeed, the emission factors determined further downwind of the source do not necessarily represent actual stack emissions. This is always not the case when emission factors show a significant dependency on transport time or distance. To make this clear and also in agreement with the following comment we introduced the term “apparent emission factor” for those EFs which undergo changes during transport and therefore do not reflect the situation at the point of emission. Those EFs which do not undergo such changes during transport are termed “emission factor” in the revised manuscript. Please see also the reply to the following comment below for further details.

I wonder whether it’d be useful to have two different terminologies: 1) emission factors for very close to the emitting ship, representing what’s coming out of the stack (=emission inventories for modelling); 2) x ratios (or named something else) that represents ’emission factors’ further downwind. This would make it clearer that the ’emission factors’ observed from a ship far away do not always represent what’s initially coming out of the stack.

Reply: We completely agree with the reviewer that the usage of two different terminologies for (1) emission factors at the point of emission and (2) emission factors as measured further downwind after atmospheric alteration would provide a clearer picture of what they really mean. Since no measurements directly at the stack of a ship have been performed we distinguish between emission factors for which we do not see a change over time after emission and which therefore can be expected to be the same at the time and point of emission as at the time when we measured them, and emission factors for which we observe a temporal change during transport of the plume. In the revised version of the manuscript we now call the former ones “emission factors” and the latter ones “apparent emission factors” throughout the text. This differentiation is introduced in section 2.4:

"In this study, emission factors are also used for the investigation of atmospheric processes (except plume dilution) and aging, which result in apparent emission factors at the point of measurement."

Some specific comments:

plume age 20 min. transported over 4 km. implies very low winds in general low winds (poor dispersion) contributes to CO2 being detectable for so long?

Reply: Indeed, most of the ship emission plumes were observed during conditions with relatively low to moderate wind speed (2 – 6 m/s, i.e. 7 – 21 km/h). However, we do not observe less efficient plume detection with increasing wind speed for plumes which were emitted at larger distance. Therefore, we do not expect a large influence of wind speed on the capability to detect a plume that was emitted at a certain distance from the measurement location. From our data, unfortunately, we cannot provide any information on the dependence of plume dispersion on wind speed.

p. 9. Evidence of enhanced OH concentrations within the plumes?

Reply: We have looked at the OH concentrations during the times when the plumes were observed in the other instruments' data sets. The concentrations observed during the plume arrival times, in comparison to those before and after these time intervals, do not show a consistent picture. We are in the process of investigating potential influencing factors which could explain the observed behavior. If successful, this could be the focus of a forthcoming publication.

Fig.3a given the small range in ambient O2 concentration (at most a few %), I'm surprised that the BC EF changes so much. does humidity affect the BC EF?

Reply: We apologize for the unclear wording in the discussion of Figure 3 which led to this misunderstanding. With "ambient oxygen concentration" we did not mean the relative contribution of oxygen to ambient air, which indeed changes only marginally, but the change in absolute concentration, i.e. number of molecules per liter. The latter one changes with increasing pressure and decreasing temperature, i.e. with increasing p/T. Further investigation of ship engine performance dependencies on ambient conditions have shown that indeed also ambient humidity does affect the combustion efficiency of such engines (see also reply to reviewer #1). To make the first point clearer and to include the information on ambient absolute humidity as requested by the reviewer, we extended Sect. 3.1 and added the EF(NOx) dependency on p/T as well as the EF(BC) and EF(NOx) dependencies on absolute humidity to Figure 3:

"Influence of combustion conditions. The ship emission plumes of the AQABA dataset enabled us to extract information regarding the influence of combustion conditions. In general, more efficient fuel combustion results in increased NO_x (especially NO) emissions owing to the enhanced oxidation of atmospheric nitrogen that occurs at higher combustion temperatures. It also leads to decreased soot particle (*here*: BC) emissions as a consequence of more efficient oxidation of fuel carbon (Corbett et al., 1999; Juwono et al., 2013; Pokhrel and Lee, 2015). The fuel combustion efficiency depends primarily on the oxygen–to–fuel mixing ratio in the combustion chamber (Khalid, 2013), but also increased ambient temperature and humidity as well as reduced ambient pressure can result in deteriorated combustion efficiencies of diesel engines, associated with elevated soot and reduced NO_x emissions (Bermudez et al., 2017; Chang et al., 2017; Rajewski, 2018). Even though the use of turbochargers and intercoolers in marine diesel engines should minimize the influence of ambient conditions onto the combustion process, we found indications for combustion efficiency dependence on such variables. With increasing ambient pressure p and decreasing temperature T, as well as for an increase in the p/T ratio (Fig. 3(a)), a reduction of the BC emission factor by more than a factor of 2 over the range of observations and a general increase of the NO_x emission factor were observed, both indications for improved combustion efficiency. Likewise, deteriorated combustion efficiency with increasing ambient humidity is suggested by the observed dependencies of the BC and NO_x emission factors on ambient water vapor concentration (Fig. 3(b))."

Fig.3b the NO:NO2 ratio depends on the reactions with O3 and so plume age. it's also probably affected by photochemistry. those complexities are not teased out in this figure. perhaps limit the analysis only to a certain plume age?

Reply: The reviewer is absolutely right: the NO/NO2 ratio depends not only on ship velocity but also on other factors like plume age as shown in Figure 7a. As mentioned above, most of the emission factors and emission ratios depend on a large number of external factors. For the NO/NO2 ratio we tried to tease out this additional dependency by color-coding the markers in the un-binned correlation depending on the plume age, associated with each individual plume event. Due to additional influences on the NO/NO2 ratio, this does not provide a conclusive picture:

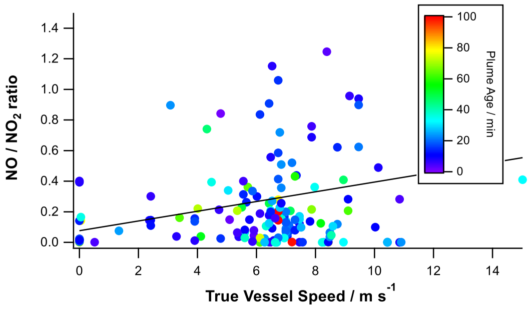

Limiting the correlation of NO/NO2 versus vessel speed to data from only one plume age would strongly reduce the number of data points. Nevertheless, there would still be a significant amount of scatter in the remaining data points in the correlation due to additional external influences on the NO/NO2 ratio.
We think the best approach to tease out the different dependencies of a certain pollutant ratio or emission factor on various influencing parameters in our case is to present several of these dependencies and provide the respective Pearson's R values to indicate which of the dependencies is the strongest one. To stress the fact that NO/NO2 does not only depend on vessel speed but also on plume age, we added a reference to Figure 7a and Section 3.3 to the discussion of Figure 3c (the former Figure 3b). In addition, we used the plume age dependence of the NO/NO2 ratio which we

obtained in Section 3.3 and used it to calculate the "initial NO/NO2 ratio", as it would have been observed close to the point of emission, for each plume. For these initial NO/NO2 ratios we also determined the vessel speed dependence (Figure S13) and added this information to Table 2. The fact that both regressions (for the measured ratios and for the calculated initial ratios) show identical slopes shows that binning of data or calculating regressions for all data largely averages out additional influences on the observables. In order to reflect this, we revised the text as follows (Sect. 3.1):

"In agreement with this, we find a 3–fold increase in the measured NO to NO_2 ratio and an almost 3–fold increase in the NO_x emission factor over the range of observed vessel speeds from 0 to ~10 m s^{-1} (see Fig. 3 (c)). Here, it must be noted that also other external parameters influence the NO to NO_2 ratio, like e.g. atmospheric processing during plume transport as shown in Section 3.3 and Figure 7a. To account for this aging effect, we calculated initial NO to NO_2 ratios for each ship emission plume (i.e. the ratio that would have been observed close to the point of emission), using the respective plume age and the plume age dependence of the NO to NO_2 ratio as provided in Table 2. The resulting dependence of the NO to NO_2 ratio on the vessel speed, taken from the correlation plots (Figure 7a and Figure S13) is provided in Table 2 for both, the observed ratios ($[NO]/[NO_2]_{obs}$) and the calculated initial ratios ($[NO]/[NO_2]_{ini}$). The slopes of both regressions are identical, showing that additional influences on this ratio largely average out when binning the data or calculating the linear fits."

Fig3. Does organic EF vary with combustion efficiency or ship velocity?

Reply: From our observations we do not see a significant dependence of the organic EF on ship velocity. While the BC EF decreases over the range of observed ship velocities by 70% of its initial value (observed at 0 m/s), no significant change of organic EF (+10% over the range of observed ship velocities with values ranging within an uncertainty interval of -13% to +33%) was observed as a function of ship velocity. However, the organics EF does depend strongly on fuel sulfur content as discussed in the manuscript (see Figure 4b).

Fig.5 as eluded to in section 3.2 the importance of coagulation on aerosol number emission also depend on the plume age to some extent. that complexity is again not teased out here

Reply: The reviewer is completely right: aerosol number emission factors do not only depend on coagulation within the exhaust system of the vessels (associated with ship size, i.e. gross tonnage), but also on coagulation within the transported plume and thus on dilution during emission into ambient air, associated with ambient wind speed (Figure 6b) and on transport time of the plume (Figure 9c). There are potentially more, albeit even smaller influences on PN emission factors like fuel quality or combustion efficiency, which are not presented here. Due to this enormous complexity of PN emission factors on many different influencing factors, we opted to present the individual dependencies of the strongest influences using correlation plots of binned data only. This averages out some of the other influences and allows focusing on the respective influence that is investigated. As an example, here we show the PN emission factor versus vessel gross tonnage (Figure 5), color-coded by plume age, as suggested by the reviewer:

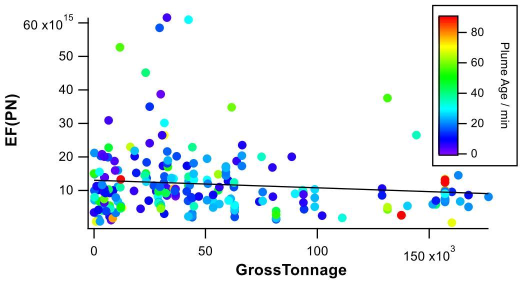

This Figure shows that including this additional information within the plot does not provide additional clarity. Averaging into bins is needed to tease out the individual dependencies. This is why we used this approach in the manuscript. In order to make this additional dependence of PN emission factors on plume age, but also on ambient wind speed clearer, we added a reference to the other two figures to the discussion of Figure 5:

"… In agreement with this, we observe a reduction in particle number EF with increasing ship size (see Fig. 5), similar to the observations by Diesch et al. (2013). Additional influences on particle number EF are caused by coagulation in ambient air, either during plume emission from the stack (section 3.2, Figure 6b) or during plume transport (Section 3.3, Figure 9c). In the correlation shown in Figure 5, these influences are largely averaged out by using binned data. *"*

Fig.6 besides coagulation and condensation, could wind speed or sea state alter the performances of the ships engines, and hence the aerosol emission factors?

Reply: Thank you for this interesting suggestion. We do not see a significant dependence of the aerosol emission factors presented in Figure 6 on vessel speed and thus on ship engine performance. Furthermore, wind speed or sea state will probably have an influence on the load of the vessel's engines; however, this influence will depend on the relative direction of the wind and the vessel movement. Since these directions are independent from each other, they will likely average out for an ensemble of vessels.

P 13 line 16. 1/3 of initial ratio? Initially it's almost all NO

Reply: We appreciate this information. Since we did not perform measurements directly at the stack, we do not have any data on the NO/NO2 ratio at the time of emission. In our measurements this ratio was 0.6 for the youngest emission plume bin, as stated in the text. To make clear that we refer to the initial ratio as the one with the shortest atmospheric transport time we re-worded the respective sentence as follows:

*"*We observe that the NO to NO_2 ratio decreases quickly down to 0.2 (i.e. one third of the ratio measured in the youngest plume age bin) during the first half hour of atmospheric transport of ship plumes emitted during daytime."

SO2/sO4 ratio decreases with humidity. Could this be partly due to cloud processing (if cloudy)?

Reply: This is an interesting point. However, we can rule out cloud processing as the reason for the decrease in SO2/SO4 ratio: We did not observe relative humidity above 90% during the ship emission plume measurements and no cloud formation; furthermore, we observed this decrease in SO2/SO4 ratio over the whole range of observed relative humidity from 40% up to 90%.

Fig9 changes in aerosol composition with aging. Would be interesting to see this separated to daytime and nighttime

Reply: We agree with the reviewer's comment that separation of the aerosol composition changes with transport time into daytime and nighttime provides additional insight into the processes. When separating the data into daytime and nighttime data for the three different plume age intervals we observe that for some species in some plume age intervals we find only a very small number of emission factors above detection limit. To avoid an excessive influence of individual very large or small values we determined the typical composition during the individual plume age intervals by calculating median (instead of average) emission factors. This changes the individual fractional contributions slightly, but does not change the overall conclusion. In addition to the total (including daytime and nighttime data) aerosol composition dependence on plume age (in Figure 9d) we also present the data separated for daytime and nighttime in the supplementary material (Figure S14). All this and some additional information were included in the discussion of Figure 9 (Sect. 3.3):
"To investigate the changes in chemical composition of the plume aerosol particles we calculated typical particle compositions for three different plume age intervals including approximately the same number of data points, using the medians of the respective emission factors: for plumes younger than 16 min, for plume ages between 16 and 40 min, and for plumes older than 40 min (see Fig. 9 (d)). The processes during plume aging are reflected in these relative compositions: The organic fraction contributes increasingly less and the inorganic fraction increasingly more to the particle phase. This is due to strong increases in the inorganic emission factors during plume transport, while the organic EF increases only very slightly. When looking separately at the plume development during day and night time, we find these effects to be much stronger during the day, compared to the night (see Figure S14), consistent with photochemical processes contributing to the formation of secondary inorganic aerosol components. We emphasise that the relatively low number of data points for some species during individual plume age intervals and large scatter of emission factors due to other influences results in some of the variability observed in the relative composition of the particle phase."

Relationship between O/C ratio and organic EF. Unclear whether 'increase in mass through Oxidation' occurs in atmosphere or in stack

Reply: Thank you for pointing this out. This statement is related to processes in the transported plume. To make this clear we revised the sentence to (Sect. 3.2):
"However, the particulate organic EF and the O/C ratio show a positive correlation (see Fig. 8 (b)), generally suggesting an increase of organic particulate mass, potentially through oxidation of gas phase organic material during plume transport."

P 18 line 19. Higher NO:NO2?

Reply: Thank you for this important hint. We corrected the respective sentence.

Influence of vessel characteristics and atmospheric processes on the gas and particle phase of ship emission plumes: In–situ measurements in the Mediterranean Sea and around the Arabian Peninsula

Siddika Celik[1], Frank Drewnick[1], Friederike Fachinger[1], James Brooks[2], Eoghan Darbyshire[2], Hugh Coe[2], Jean–Daniel Paris[3], Philipp G. Eger[4], Jan Schuladen[4], Ivan Tadic[4], Nils Friedrich[4], Dirk Dienhart[4], Bettina Hottmann[4], Horst Fischer[4], John N. Crowley[4], Hartwig Harder[4], and Stephan Borrmann[1,5]

[1]Particle Chemistry Department, Max–Planck–Institute for Chemistry, Mainz, 55128, Germany
[2]Centre for Atmospheric Science, University of Manchester, Manchester, M13 9PL, UK
[3]Laboratoire des Sciences du Climat et de l'Environnement, CEA–CNRS–UVSQ, Gif–sur–Yvette, 91191, France
[4]Atmospheric Chemistry Department, Max–Planck–Institute for Chemistry, Mainz, 55128, Germany
[5]Institute for Atmospheric Physics, Johannes Gutenberg University Mainz, Mainz, 55128, Germany

Correspondence to: Frank Drewnick (frank.drewnick@mpic.de)

Abstract. 252 emission plumes of ships operating in the Mediterranean Sea and around the Arabian Peninsula were investigated using a comprehensive dataset of gas and submicron particle phase properties measured during the two–month shipborne AQABA field campaign in summer 2017. The post–measurement identification of the corresponding ship emission events in the measured data included the determination of the plume sources (up to 38 km away) as well as of the plume ages (up to 115 min) and was based on commercially available historical records of the Automatic Identification System. The dispersion lifetime of chemically inert CO_2 in the ship emission plumes was determined as (70 ± 15) min, resulting in levels indistinguishable from the marine background after (260 ± 60) min. Emission factors (EFs) as quantities that are independent of plume dilution were calculated and used for the investigation of influences on ship emission plumes caused by ship characteristics and the combustion process as well as by atmospheric processes during the early stage of exhaust release and during plume aging. Combustion efficiency and therefore emission factors of black carbon and NO_x were identified to depend mostly on the vessel speed and gross tonnage. Moreover, larger ships, associated with higher engine power were found to use fuel with higher sulfur content and have higher gas phase SO_2, particulate sulfate, particulate organics and particulate matter EFs. Despite the independence of EFs on dilution, significant influence of the ambient wind speed on the particle number and mass EFs was observed that can be traced back to enhanced particle coagulation in case of slower dilution and suppressed vapor condensation on particles in case of faster dilution of the emission plume. Atmospheric reactions and processes in ship emission plumes were investigated that include NO_x and O_3 chemistry, gas–to–particle conversion of NO_x and SO_2 and the neutralization of acids in the particle phase through the uptake of ambient gas phase ammonia, the latter two of which cause the inorganic particulate content to increase and the organic fraction to decrease with increasing plume age. The results ~~enable identification of the most important influences on (or processes in) ship emission plumes and~~allow to describe ~~those~~ the

influences on (or processes in) ship emission plumes quantitatively by parameterizations, which could be used for further refinement of atmospheric models, and to identify which of these processes are the most important ones.

1 Introduction

Globalization and international trade as one of its essential components are expected to grow in the longer term. Currently, ships are carrying about 90 % of the world's trade by volume (Smith et al., 2015). This is mainly due to cost reasons, because ships are considered as energy efficient means of transport of passengers and goods in comparison to on–road vehicles and aircraft (Jonsson et al., 2011). Thus, shipping represents an indispensable and expanding mode of transport as an international economic factor (Chen et al., 2018).

Historically, there was no extensive, legislative regulation of air pollutant emissions caused by maritime traffic, as (ocean–going) ships operate most of their time far away from areas of human habitation (Juwono et al., 2013; Moldanová et al., 2013). Therefore, especially large ocean–going vessels burn inexpensive residual diesel fuel as cost saving measure (Juwono et al., 2013). This fuel usually has a high sulfur content of up to 4.5 wt. %, whereas the sulfur content of diesel fuel used for the road traffic in most European countries is 4500 times lower, i.e. 10 ppm(m) (Fridell et al., 2008). In this context, since 1973 the International Maritime Organization (IMO) sets binding and periodically tightened regulations for maritime pollutant emissions with the MARPOL convention. Special legally binding restrictions for the emissions of NO_x (= $NO + NO_2$) and SO_x (= $SO_2 + SO_3$) as well as of particulate matter (PM) caused by ships exist for so–called Emission Control Areas (ECAs) (IMO, 2019). However, concerning environmental protection these regulations are not yet extensive enough. On a global scale approximately 2.2 % of anthropogenic CO_2 emissions, 15 % of anthropogenic NO_x emissions and 5 to 8 % of anthropogenic SO_x emissions are related to ocean–going vessels (Corbett et al., 2007; Nunes et al., 2017; Metz et al., 2007).

Considering the significant anthropogenic influence of shipping on the atmosphere on a regional and global scale and the associated negative influences on air quality and climate, the investigation of the gas and particle phase of ship emission plumes gains increasing importance from both ecological and epidemiological points of view (Diesch et al., 2013; Juwono et al., 2013). In the literature, experimental studies can be classified as follows:

- Exhaust sampling of a large number of operating vessels from stationary (e.g. at harbors or shore sites) or mobile (e.g. research vessel or aircraft) measurement platforms (e.g. Williams et al., 2009; Jonsson et al., 2011; Alföldy et al., 2013; Diesch et al., 2013);
- Multiple sampling and tracking of the emissions of few individual operating vessels using a research vessel or aircraft (e.g. Sinha et al., 2003; Chen et al., 2005; Cappa et al., 2014);
- On–board studies conducted on an operating vessel (e.g. Agrawal et al., 2008; Moldanová et al., 2009, 2013);
- Measurements with a test rig in a laboratory (e.g. Petzold et al., 2008).

These studies give a broad overview of emission factors (EFs) and their variability for a variety of species of the aerosol gas and particle phase. EFs refer the quantity of emitted species to the amount of burned fuel and are therefore independent of the emission plumes' dilution. However, so far these investigations neither provide an extensive knowledge of the parameters causing the observed variability nor on the extent to which these parameters affect the emissions. On–board and test rig studies could be partially exempted from this statement, but they do not offer information on ship emission plumes on a large selection of ships or under real–world conditions, respectively. Moreover, previous experimental studies provide little information on atmospheric processing and aging of ship emission plumes because in most cases ship emission plumes were investigated that were emitted at less than 5 km distance and were less than 15 min old when reaching the measurement site (Alföldy et al., 2013; Diesch et al., 2013). In addition, the measurement conditions in these studies (e.g. time of day, meteorology, ships' operating conditions, etc.) only vary to a minor extent. Furthermore, previous studies usually cover a small number of species in ship emission plumes, which makes it difficult to investigate processes running in parallel that can be traced to the same cause (e.g. to atmospheric aging or to the combustion process).

The AQABA (Air Quality and climate change in the Arabian BAsin) field campaign provides an extensive and diverse dataset to investigate ship emission plumes, emitted at various horizontal distances to the measurement location and therefore of different ages. For a variety of species of the aerosol gas and particle phase data have been collected on–board the research vessel *Kommandor Iona* during this two–month field campaign in summer 2017. The research vessel's route led from Southern France through the Mediterranean Sea and around the Arabian Peninsula to Kuwait and the same way back. Given the large geographic and temporal coverage of the field campaign the dataset contains information on emissions of a diversity of vessels of different size, speed, type, etc. that were measured under various atmospheric conditions regarding meteorology and solar radiation.

The aim of this study is to investigate ship plumes emitted in the Mediterranean Sea and around the Arabian Peninsula using time–resolved measurements of aerosol gas and particle phase species that were recorded during the AQABA field campaign. For this purpose, ship emission plumes were determined and characterized according to their age, transport distance, and source vessel using historical Automatic Identification System (AIS) data. Plume quantities of identified ship emission plumes, especially EFs, were calculated in order to investigate them with respect to the following influencing parameters:

- **Fuel quality**: How does the fuel sulfur content influence the quantity of emitted species?
- **Ship parameters and combustion process**: How does e.g. the ship velocity (and thus the engine load) affect the combustion efficiency? What are the effects of the exhaust system's size and thus of the exhaust's residence time in it?
- **Meteorology and solar radiation**: How do atmospheric dilution, transport, and aging affect the characteristics of ship emission plumes?

2 Experimental methods

2.1 AQABA field campaign

The AQABA field campaign took place from 24 June to 03 September 2017 on the research vessel *Kommandor Iona* that served as measurement platform. Figure 1 shows the route of the research vessel during the field campaign. The first leg started at the seaport of Toulon, proceeding consecutively through the Mediterranean Sea, the Suez Canal, the Red Sea, the Gulf of Aden, the Arabian Sea, the Gulf of Oman and the Persian Gulf and ended on 31 July when reaching the harbor of Kuwait. The second leg included the reverse route from Kuwait back to Toulon. Time series for a variety of species of the aerosol gas and particle phase were measured with high time resolution (between 1 s and 1 min depending on the measured variable), including both background air and events from individual ship emission plumes. The main objectives of the AQABA field campaign were to gain knowledge on the influences of natural and anthropogenic emissions on air quality and climate and to investigate the interaction of the terrestrial and marine ecological systems.

2.2 Instrumentation for shipborne in–situ measurements during AQABA

For the purpose of the AQABA field campaign five measurement containers equipped with measurement instruments were installed on the *Kommandor Iona* and the sampling of outdoor air was realized through appropriate inlet systems for each of the instruments. Table 1 gives an overview of the measurement instruments that were used for this study. In general, the processing of data (timestamp: UTC) included calibrations, corrections (e.g. of the time delay due to the transport time of sampled air through the inlet system), the removal of unusable data (e.g. due to malfunctioning instruments) and the removal of data contaminated by sampling the ship's own exhaust. All presented particle and gas phase data were scaled to a pressure of $p = 1013.25$ hPa and a temperature of $T = 20$ °C.

Particle phase measurements. The instruments used to measure particle phase data are described in detail by Drewnick et al. (2012). For the measurement of aerosol particles, a self–regenerating silica gel aerosol dryer with two parallel, switchable columns was integrated between the sampling inlet, located approximately 12 m above sea level, and the corresponding instruments. One of the columns was in use to dry the sampled ambient aerosol (relative humidity (RH) behind the aerosol dryer was typically ≤ 40 %), while the other one was regenerated at the same time by heating and flushing it with dry air. The sampling through the columns was switched between the two once per day. Particle loss due to the whole inlet system, estimated for the relevant size ranges (see Table 1; von der Weiden et al., 2009), was largely negligible. Concentrations of non–refractory submicron particle chemical components, namely particulate sulfate ($\mathrm{SO_4^{2-}}$), particluate nitrate ($\mathrm{NO_3^-}$), particulate ammonium ($\mathrm{NH_4^+}$), particulate chloride ($\mathrm{Cl^-}$), and total particulate organics, were determined with a High–Resolution Time–of–Flight Aerosol Mass Spectrometer (HR–ToF–AMS; DeCarlo et al., 2006) using the medium mass resolution mode ("V–mode") with 30 s time resolution. The ionization efficiency of the instrument as well as the relative ionization efficiencies of $\mathrm{SO_4^{2-}}$ and $\mathrm{NH_4^+}$ were determined via regular calibrations throughout the campaign. The atomic O/C and H/C ratios were calculated according to Aiken et al. (2008) using the high–resolution mass spectra. Averaged data with 10 s time resolution were used in case of all following particle phase data. An Aethalometer measured black carbon (BC) concentrations in PM_1 via light absorption ($\lambda = 880$ nm) through on–line filter sampled aerosol particles. Due to malfunctions, the instrument was exchanged for an identical one once during the field campaign. A default C–factor of 1.57 was applied to account for multiple scattering within the filter (Drinovec et al., 2015). Temperature fluctuations due to the on– and off–switching of the air conditioning system in the measurement container caused periodic fluctuations of the measured BC concentration. These fluctuations were taken into account by always averaging over full fluctuation periods when calculating average concentrations as described in Sect. 2.4. Polycyclic aromatic hydrocarbon (PAH) mass concentrations on PM_1 particles were detected with a PAH monitor. Particle number concentrations (PNCs) are given both by an ultrafine water–based Condensation Particle Counter (CPC) and by the integrals of the size resolved PNCs over the whole size range of a Fast Mobility Particle Sizer (FMPS). PNCs used for this study were calculated by averaging the data from both instruments. In addition, the FMPS provides the particle number size distributions. As the ship emission plumes measured during the AQABA field campaign showed particles exclusively in the (lower) size range of the FMPS, this data was used to calculate PM_1 particle mass concentrations from the FMPS-derived total particle volume concentration (V_{FMPS}), assuming spherical particles and an average particle density of 1.53 g cm^{-3} calculated using the mass concentrations of AMS species and BC (ρ_{AMS+BC}). The calculated PM_1 particle mass concentrations were corrected for under–measurement in the upper size range of the FMPS (> 130 nm; Levin et al., 2015) by scaling them with a factor of F_{corr}=1.85, which was derived from comparison with size distribution data from a concurrently measuring Optical Particle Counter (OPC, Grimm Model 1.109):~~.~~

$$PM_1 = V_{FMPS} \cdot \rho_{AMS+BC} \cdot F_{corr} \qquad (1)$$

While V_{FMPS} are actually measured data for each plume event, F_{corr} and ρ_{AMS+BC} are the average correction factor for the under-measurement in the upper FMPS channels and the average particle density, determined from AMS and BC measurements for the whole field campaign. The overall uncertainty of the resulting PM_1 concentrations is estimated to be 35%. Main modes of the number size distributions were found to be exclusively in the lower size range (< 130 nm; see Sect. 3.2) and were therefore not affected by the under–measurement in the larger size bins.

Gas phase measurements. CO and CO_2 concentrations were detected by means of a Cavity Ring–Down Spectrometer (CRDS) calibrated with cylinders bracketing ambient concentrations and traceable to WMO standards. An Iodide Chemical Ionization Quadrupole Mass Spectrometer (Iodide CI–QMS) was used to measure SO_2 concentrations (Eger et al., 2019). An ozone monitor was used to detect O_3 concentrations based on light absorption at 254 nm, and a formaldehyde monitor to detect HCHO concentrations based on the Hantzsch reaction (Nash, 1953). NO and NO_2 concentrations were measured with a Two–Channel Chemiluminescence Detector (Two–Channel CLD, modified version of the commercial instrument; see Table 1). NO_x mixing ratios were detected by a Two–Channel Thermal Dissociation CRDS which is a modified version of the instrument described by Thieser et al. (2016). Some of the gas phase data, especially those of the nitrogen oxides, show periodic gaps of 1 to 2 min duration due to periodic background measurements or calibrations. These affected in some cases the detected ship emission events. ~~and, i~~If possible,~~ were taken into account by reconstructing~~ the affected events were reconstructed using the remaining parts of the times series ~~according to its shape~~ by either linear or Gaussian fits, depending on the expected shape of the missing part of the peak.

Auxiliary data. A shipborne automatic weather station provided meteorological quantities (ambient temperature T, atmospheric pressure p, wind speed, wind direction and RH) as well as via GPS the geographic location of the research vessel. A CCD spectral radiometer provided the photolysis rate constants $J\mathrm{O}^1\mathrm{D}$ (Meusel et al., 2016).

2.3 Identification and determination of ship emission plumes, their sources and ages

Since ships are point sources of pollutant emissions and usually the closest sources on the open sea, transient concentration peaks of a few minutes' duration in the AQABA dataset were considered to be potential ship emission events. The AQABA dataset contains a total of 815 of these potential single ship emission events for which the measurement locations (longitude and latitude) and measurement times were determined referring in each case to the event maximum. Using this data, commercially available historical AIS data were requested from MarineTraffic (MarineTraffic, 2019) in order to try to identify the vessels that caused the emission events (see Fig. 2). For this purpose, data on all vessels were requested which were in a 40 km × 40 km area around the measurement location during a time frame of $\pm$ 15 min around the peak observation time. Two AIS records were requested for each of these vessels, the first one complying with the time and location restrictions and as close as possible to the measurement time and the second "previous" one being recorded at least 20 min beforehand. The second AIS record was included to check the consistency of a vessel's track within the box determined by its velocity and course (i.e. all of the following calculations were perfomed for both AIS records of each ship candidate and the end results were compared). Besides that, a "previous" vessel position might be closer to the sought emission time as the emission of a plume occurs earlier than its detection. The requested AIS records included the following information: vessel identification number (Maritime Mobile Service Identity, MMSI), date and time, as well as vessel position, speed and course. From the MMSI numbers of identified ships vessel parameters like vessel name, type, gross tonnage (GT, a dimensionless measure for the vessel size) and engine power were obtained from the databases of MarineTraffic (MarineTraffic, 2019), FleetMon (FleetMon, 2019) and Equasis (Equasis, 2019).

For 648 of the 815 potential ship emission plumes a total of about 20 000 AIS records were available according to the restrictions. The identification of the vessel corresponding to a potential ship emission event by using these AIS vessel data was done with the aid of a self–developed software tool, which performed all routine calculations (see supplement, Sect. S1) to reduce the manual effort and avoid routine calculation errors.

In a first step, average wind data were calculated for each event using the meteorological quantities recorded on–board the *Kommandor Iona*. An averaging interval of 5 min was applied for the analysis. Additionally, averaging intervals of 3 min and 10 min were used for checking the consistency of results for the below described calculations; in case of inconsistent average wind data and therefore inconsistent results the potential ship emission event was not further analyzed. The average wind speed was given by the arithmetic mean and the average wind direction was calculated according to directional statistics (Eq. (S1); Mardia and Jupp, 2000). As the raw data points of both the wind speed and direction were considered as error–free, the uncertainty of the average wind speed was given by the standard deviation and the uncertainty of the average wind direction through Gaussian error propagation of Eq. (S1).

In a next step, the position where the track of the probed air mass (assuming to arrive from the average wind direction) intersects the (past or future) track of the vessel candidate (see Fig. 2) was calculated by means of trigonometric navigational equations (Veness, 2019; Tseng and Chang, 2014; Eqs. (S2) to (S12)). For this purpose, the earth was approximated as a sphere and the air mass and the potential source vessel were assumed to move on a great circle, respectively (see Fig. S1). The right intersection point (out of the two possible) of these two great circles is the one closer to the measurement location.

With this potential emission site (the intersection point calculated as above) the distances to the measurement location and to the record position of the considered AIS data point were calculated by means of the Haversine formula (Eq. (S13); Veness, 2019). Using these distances, the wind and vessel speed, the measurement time and the record time of the AIS data point, the times were calculated when the air mass and the vessel candidate were at the intersection point. The time when the air mass was at the intersection point has an uncertainty (calculated via Gaussian error propagation) which is mainly due to the uncertainty of the wind speed. The main uncertainty associated with the time when the vessel was at the intersection point is related to the uncertainty in the wind direction and is given by the time required for the vessel to pass the calculated wind sector (wind direction ± uncertainty, white area in Fig. 2). In the case that both time intervals (for air mass and vessel at the intersection point) overlap, the candidate vessel was identified as the source of an emission event and the determination of the age and travel distance of the ship's emission plume was possible. Exceptional cases, namely the case of a stationary vessel (e.g. at anchor), the case of a ship course that was (anti–)parallel to the wind direction and the case of wind velocities close to zero, were taken into consideration (see supplement for details). Individual uncertainties for both the ages and the transport distances of ship emission plumes were estimated from the uncertainties described above and the discrepancy between the results of these calculations for the two AIS records of the identified ship. In general, smaller uncertainties were found for the transport distance (on average 16 %) than for the age (on average 20 %) as the distance was fixed by the vessel track in one direction, whereas the variability of the wind speed affects directly the uncertainty of the determined age of a ship emission plume.

Out of the initially 815 potential ship emission events it was possible to determine the source vessel for 252 ship emission events (see Fig. 1), whereas 156 of these were sampled during daylight hours and 96 during night–time. There are several reasons for unsuccessful ship identifications: the identification of more than one vessel as potential source in areas with high vessel density, the lack of AIS data on vessels (e.g. in areas where only satellite AIS data with little time resolution are available, because vessels had turned off their AIS signal due to piracy, or because of missing MMSI numbers in case of e.g. small fishing vessels), or other nearby emission sources (e.g. coastal industrial plants, offshore oil rigs). The identified ship emission plumes had an age between 1 min and 115 min and were transported less than 1 km up to 38 km (see Fig. S3); the most frequently encountered plumes had an age of about 20 min and were transported about 4 km. 22 % of the identified ships were oil tankers (world fleet: 11 %), 14 % bulk carriers (world fleet: 12 %), 19 % container vessels (world fleet: 5 %), 8 % general cargo vessels (world fleet: 21 %) and 37 % other types of vessels (world fleet: 51 %) (data for world fleet from

UNCTAD, 2019). Due to regional economic conditions especially oil tankers and container vessels were observed more frequently compared to the world fleet, whereas small vessels falling into the category of other types of vessels were found less frequently probably because of missing AIS identification.

2.4 Quantification of plume characteristics

Quantification of characteristics of ship emission plumes was performed using a software tool that was written to perform all calculations, reducing the manual effort and the risk of mistakes.

The average excess (above atmospheric background) concentrations of the particle number and mass as well as of the species listed in Table 1 were calculated for the 252 ship emission events that were identified. For each ship emission event, two background intervals, one before and one after the event, and one interval including the event itself, were defined (see Fig. S4 for a graphical illustration), with interval limits set as close as possible to the event and with approximately equal interval lengths. This was achieved by comparing the event in each variable's time series to the event in the time series of the PNC, which is the most complete and significant one regarding the identified ship emission events. Accordingly, the intervals have the same width for each measured quantity of an emission event but differ in adjustments due to minor time shifts. The mean background was ~~linearly interpolated between~~calculated from the average values derived for the two background intervals and subtracted from the average event concentration to obtain the average excess concentration in the plume. Periodic fluctuations of the measured BC concentration and data gaps during a ship emission event were taken into account as described in Sect. 2.2. In general, calculated average excess concentrations below the detection limit ($LOD = \frac{3\,\sigma_{bg}}{\sqrt{n}}$, with σ_{bg} ~~defined as three times~~ the standard deviation of the background and n ~~divided by the square root of~~ the number of measurement points within the ship emission event interval) were excluded from further analysis.

The average excess concentration of a species or the particle number or mass concentration in an expanding ship emission plume changes with time in the first place due to dilution (Petzold et al., 2008; Kim et al., 2009). Emission factors that are independent of the dilution were calculated following Eq. (2~~1~~) (Diesch et al., 2013):

$$\mathbf{EF}_x = \frac{[x]}{[\mathbf{CO_2}] \cdot \frac{M_\mathbf{C}}{M_\mathbf{CO_2}}} \cdot \boldsymbol{w}_\mathbf{C},$$
(~~1~~2)

where x is the excess quantity of a gas or particle phase species, $M_\mathrm{C}/M_{\mathrm{CO}_2}$ the carbon mass fraction in CO_2 and $w_\mathrm{C} = 0.865$ kg C (kg fuel)$^{-1}$ (Diesch et al., 2013) the mass fraction of carbon in marine diesel fuel. EF_x is given in g or number per kg of burned fuel, $[x]$ is in µg per m^3 in case of mass concentrations (NO_x is given as NO_2) and in 10^{12} # per cm^3 in case of number concentrations, and $[CO_2]$ is in mg per m^3. Here, it is assumed that both x and CO_2 experience dilution in the same way and that the concentration of chemically inert CO_2 in an expanding ship emission plume is affected exclusively by plume dilution, so that it remains proportional to the amount of burned fuel (Corbett et al., 1999). Furthermore, it is assumed that fuel carbon is completely emitted as CO_2 (CO_2 balance method), i.e. that the fraction of other carbon species like CO, CH_4, volatile organic compounds (VOCs) and particulate carbon in a ship emission plume is negligible compared to CO_2. The amount of x is referred in the EF to the amount of burned fuel via the mass fraction of carbon in marine diesel fuel (Diesch et al., 2013; Sinha et al., 2003). Strictly speaking, emission factors should refer to the time of emission which is possible only in case of conservative plume characteristics that do not change during plume expansion in the atmosphere (Petzold et al., 2008). In this study, emission factors are also used for the investigation of atmospheric processes (except plume dilution) and aging, which result in apparent emission factors at the point of measurement.

Based on the exponential decrease of the average excess concentration of CO_2 during the expansion of the ship emission plumes an average plume dispersion time constant (i.e. the e-folding time) of (70 ± 15) min was determined (see Fig. S5 for $[CO_2](t)$). From the decrease in excess CO_2 concentration during transport it takes on average (260 ± 60) min to reach the detection limit of the excess CO_2 concentration, i.e. the time required for the plume to become indistinguishable from the background. Chen et al. (2005) report that plume dispersion results in a ship's emission event older than 3 h being indistinguishable from the background level, in good agreement with our findings. According to Petzold et al. (2008) it takes less than 24 h until a ship emission plume is completely mixed with the marine boundary layer (MBL).

Average particle number size distributions of ship emission plumes were calculated proceeding in the same way as for calculating average excess concentrations and using the same background and ship emission event intervals as for the PNC. From log–normal fits to the resulting excess particle number size distributions, in each case the count median diameter (CMD), the geometric standard deviation (GSD) and the width of the distribution, referring to one geometric standard deviation, were obtained. The determination of the width followed Eq. (~~2~~3) (Hinds, 1999):

$$\mathbf{width} = \mathbf{CMD} \cdot \left(\mathbf{GSD} - \mathbf{GSD^{-1}}\right).$$

(~~2~~3)

We define here the expression "potential photochemical processing" of the ship emission plume as the product of the average measured photolysis rate JO^1D during the plume transport and the plume age (t) $(\rightarrow JO^1D \cdot t)$ in Hz·s, which is used as a proxy for potential photochemical processing of plume components in the atmosphere. The relative uncertainty of this quantity is on average 27 % considering the average relative uncertainty of the plume age and the relative measurement uncertainty of JO^1D. Measured OH concentrations were not used as a measure of photochemical processing due to insufficient data coverage and because they are more affected by local influences than the photolysis rate and therefore more so than the latter describe merely the situation at the research vessel's position rather than within the plume. A better measure for photochemical processing would be the modelled OH concentrations along the plume transport path. However, this modelling is well beyond the scope of this work.

Using the measured mass concentrations of particulate organics ([organics]) and the atomic O/C and H/C ratios for the organic aerosol during plume and background measurements, the O/C ratios for the plume contribution were calculated (Eq. 6~~5~~) ~~via~~ from the average mass concentrations of oxygen and carbon for both the background (B) and for the ship emission event (emission + background, EB). The mass concentrations of O and C were calculated from the mass fraction of oxygen and carbon in the organic aerosol, determined from the measured atomic O/C and H/C ratios, following Eqs. (4~~3~~) and (5~~4~~):

$$[\mathbf{O}] = \frac{[\mathbf{organics}]\cdot \boldsymbol{m}_\mathbf{O}}{\boldsymbol{m}_\mathbf{O}+\boldsymbol{m}_\mathbf{H}+\boldsymbol{m}_\mathbf{C}} = \frac{[\mathbf{organics}]\cdot \mathbf{O/C}\cdot \boldsymbol{M}_\mathbf{O}}{\mathbf{O/C}\cdot \boldsymbol{M}_\mathbf{O}+\mathbf{H/C}\cdot \boldsymbol{M}_\mathbf{H}+\mathbf{C/C}\cdot \boldsymbol{M}_\mathbf{C}},$$

(~~3~~4)

$$[\mathbf{C}] = \frac{[organics]\cdot m_C}{m_O + m_H + m_C} = \frac{[\mathbf{organics}]\cdot \boldsymbol{M}_\mathbf{C}}{\mathbf{O/C}\cdot \boldsymbol{M}_\mathbf{O} + \mathbf{H/C}\cdot \boldsymbol{M}_\mathbf{H} + \boldsymbol{M}_\mathbf{C}},$$ (~~4~~5)

$$\mathbf{O/C} = \frac{([\mathbf{O}]_\mathbf{EB} - [\mathbf{O}]_\mathbf{B})/\mathbf{M_O}}{([\mathbf{C}]_\mathbf{EB} - [\mathbf{C}]_\mathbf{B})/\mathbf{M_C}},$$ (~~5~~6)

where m_x is the (measured) total mass and M_x the atomic weight of the respective species x. For these calculations we assume that particulate organics consist only of oxygen, hydrogen and carbon. To check for consistency, the H/C ratio was calculated analogously and found to always show the expected reverse behaviour to the O/C ratio.

The fuel sulfur content (wt. % fuel S) was calculated according to Diesch et al. (2013) by using the EFs of SO_2 and SO_4^{2-} and assuming that the fraction of other sulfur species like SO_3 and gas phase H_2SO_4 is negligible in the ship emission plumes.

The modified combustion efficiency was calculated based on the approximation that the fraction of carbon species like CH_4, VOCs and particulate carbon in a ship emission plume is negligible compared to CO_2, so that the modified combustion efficiency is given by the ratio of the average excess CO_2 concentration to the sum of the average excess concentrations of CO_2 and CO (Ward and Radke, 1993).

Frequency distributions of all calculated quantities are given in Fig. S6.

3 Results

Parallel measurements of multiple variables which are associated with ship emission plumes and observation of such plumes under very different conditions (e.g. plume age, meteorological conditions, source vessel characteristics, etc.) allow the investigation of factors which might influence the characteristics of ship emission plumes. For this purpose, we investigated the relationship between plume characteristics and various factors (above mentioned measurement conditions) by correlation analysis, which, contrary to Lagrangian measurements of individual ship plumes during transport away from the source, provide ensemble-averaged information on emission or transformation characteristics of plume properties. As several different factors can influence individual plume characteristics, the correlation plots always show a relatively strong degree of scatter, which led us to bin them, such that the same number of data points (at least 5 and maximal 32) was included in each bin, resulting in not equidistantly distributed bins. The slope and~~,~~ intercept~~, and correlation coefficient~~ did not significantly change when using binned data instead of raw data. Therefore, fit parameters for the correlation of raw data are presented in Table 2, while in the figures usually the binned data are shown for clarity. In case raw data are presented their relative uncertainties combine the estimated quantification (Sect. 2.4) and measurement uncertainties, whereas in case of binned data error bars include in addition one sigma standard deviations of the data distributions in each bin. Using bin-averaged data or linear regressions strongly reduces the influence of additional influencing factors on the individual data points and, to a large degree, provides information on the dependence of the respective plume feature on the influencing factor under investigation. To extract the influence of several influencing external factors on plume characteristics, separate correlation plots for each of these factors were therefore generated.

In the following sections we first discuss the influences of ship–related properties on the emission characteristics before we present the influences of the early stage of expansion and of chemical processing during transport. Finally, we use averages of emission factors for comparison with data from the literature.

3.1 Influences of ship properties and the combustion process on ship emission plumes

Influence of combustion conditions. The ship emission plumes of the AQABA dataset enabled us to extract information regarding the influence of combustion conditions. In general, more efficient fuel combustion results in increased NO$_x$ (especially NO) emissions owing to the enhanced oxidation of atmospheric nitrogen that occurs at higher combustion temperatures. It also leads to decreased soot particle (*here*: BC) emissions as a consequence of more efficient oxidation of fuel carbon (Corbett et al., 1999; Juwono et al., 2013; Pokhrel and Lee, 2015). The fuel combustion efficiency depends primarily on the oxygen–to–fuel mixing ratio in the combustion chamber (Khalid, 2013), but also increased ambient temperature and absolute humidity as well as reduced ambient pressure can result in deteriorated combustion efficiencies of diesel engines, associated with elevated soot and reduced NO$_x$ emissions (Bermudez et al., 2017; Chang et al., 2017; Rajewski, 2018). Even though the use of turbochargers and intercoolers in marine diesel engines should minimize the influence of ambient conditions onto the combustion process, we found indications for combustion efficiency dependence on such variables. With increasing ambient pressure p and decreasing temperature T, as well as for an increase in the p/T ratio (Fig. 3(a)), a reduction of the BC emission factor by more than a factor of 2 over the range of observations and a general increase of the NO$_x$ emission factor were observed, both indications for improved combustion efficiency (see below). Likewise, deteriorated combustion efficiency with increasing ambient absolute humidity is suggested by the observed dependencies of the BC and NO$_x$ emission factors on ambient water vapor concentration (Fig. 3(b)).~~This ratio can be influenced by various factors. We found a strong dependence of the BC emission factor on the ambient oxygen concentration: With increasing ambient pressure–to–temperature ratio (i.e. increasing oxygen concentration according to the ideal gas law) the BC emission factor decreased by more than a factor of 2 over the range of observations, likely due to improved combustion efficiency (see Fig. 3 (a)).~~

Another important parameter for combustion efficiency is the combustion temperature: With increasing combustion temperature, combustion is more efficient, but more nitrogen oxides are produced. Furthermore, reduced oxidation of NO to NO$_2$ in the oxygen–deficient exhaust gas, which occurs after efficient combustion in the propulsion system, results in an increase of the NO to NO$_2$ ratio with increasing combustion efficiency (Rößler et al., 2017). According to the literature, a higher vessel speed, engine load, or engine power causes a higher peak combustion temperature in the engine system and thus more efficient fuel combustion (Cappa et al., 2014; Sinha et al., 2003). In agreement with this, we ~~observe~~ find a 3–fold increase in the measured NO to NO$_2$ ratio and an almost 3–fold increase in the NO$_x$ emission factor over the range of observed vessel speeds from 0 to ~10 m s^{-1} (see Fig. 3 (c~~b~~)). Here, it must be noted that also other external parameters influence the NO to NO$_2$ ratio, like e.g. atmospheric processing during plume transport as shown in Section 3.3 and Figure 7a. To account for this aging effect, we calculated initial NO to NO$_2$ ratios for each ship emission plume (i.e. the ratio that would have been observed close to the point of emission), using the respective plume age and the plume age dependence of the NO to NO$_2$ ratio as provided in Table 2. The resulting dependence of the NO to NO_2 ratio on the vessel speed, taken from the correlation plots (Figure 7a and Figure S13) is provided in Table 2 for both, the observed ratios ($[NO]/[NO_2]_{obs}$) and the calculated initial ratios ($[NO]/[NO_2]_{ini}$). The slopes of both regressions are identical, showing that additional influences on this ratio largely average out when binning the data or calculating the linear fits.

As a consequence of improved combustion, the BC emission factor also decreased to a similar degree as the NO to NO_2 ratio, acquiring at a vessel speed of 10 m s^{-1} about one third of the value at 0 m s^{-1}. On–board electric power is usually generated by an auxiliary engine, which results in emissions from stationary vessels ($v_{\mathrm{ship}} \sim 0$ m s^{-1}) (Pokhrel and Lee, 2015; Williams et al., 2009). For very slow vessels, the relative contribution of this auxiliary engine to the overall emissions becomes especially significant.

While a similar dependence of the NO_x emission factor on the engine power was observed (presented in the supplement in Fig. S7) the dependence of combustion efficiency–related EFs on ship size (gross tonnage) is more complex. While for small ships the combustion efficiency seems to increase (increasing NO_x EF, decreasing BC EF) with increasing gross tonnage, which was also observed by Diesch et al. (2013) and Williams et al. (2009), a plateau is reached at about a gross tonnage of 50 000, and for very large vessels (GT > 150 000) the combustion efficiency seems to deteriorate again without any obvious reason (see Fig. 3 (d~~c~~)). For vessels in the optimum size range the better combustion efficiency, compared to the very small ships, results in about 50 % lower BC emissions and more than doubled NO_x emissions per kg of burned fuel.

Influence of fuel quality. The influences of fuel quality on ship emission plumes were investigated with regard to fuel sulfur content. Diesel fuel used for shipping is in general a blend of refined fuel and residual oil (Mohd Noor et al., 2018). For economic reasons, large ocean–going vessels often burn cheap heavy fuel oil (HFO) that is highly contaminated with sulfur, ash, asphaltenes, and metals (Corbett et al., 1999; Buffaloe et al., 2014). High quality but expensive marine gas oil (MGO) and marine diesel oil (MDO) are usually only used for the operation of small vessels and vessels operating in ECAs or in coastal areas (Buffaloe et al., 2014; Cappa et al., 2014). Our dataset suggests a general increase of the fuel sulfur content, calculated from the emission factors of SO_2 and SO_4^{2-}, with increasing ship size (see Fig. 4 (a)), and therefore more frequent usage of cheap HFO fuel in the larger vessels.

In order to minimize corrosive effects from the high sulfur content in the fuel, ship engine systems are designed to operate at high exhaust flow rates and temperatures, avoiding formation of SO_3, condensation of water vapor and formation of sulfuric acid (Pirjola et al., 2014; Moldanová et al., 2009). Furthermore, lubricating oil serves not only as protection against wear but also as neutralizer for corrosive species like sulfuric acid in the exhaust system. For these reasons, lubricating oil consumption, and as a consequence emission of organic particulate matter, depends on fuel quality (Lack et al., 2009; Juwono et al., 2013; Cappa et al., 2014; Chu–Van et al., 2018). We found almost a doubling of organic aerosol EFs (and of total PM_1 EFs) over the range of observed fuel sulfur contents from 0.5 to 2.5 wt. % (see Fig. 4 (b)), showing the significant indirect influence of fuel sulfur content on ship emission characteristics.

Coagulation in the exhaust system. Generally, coagulation of particles, which reduces particle number concentrations without changing particle mass concentrations, occurs more efficiently at higher particle number concentration levels. Longer residence times within the exhaust system, as they typically occur in larger ships, should therefore result in lower particle number concentrations due to enhanced coagulation effects. In agreement with this, we observe a reduction in particle number EF with increasing ship size (see Fig. 5), similar to the observations by Diesch et al. (2013). Additional influences on particle number EF are caused by coagulation in ambient air, either during plume emission from the stack (section 3.2, Figure 6b) or during plume transport (Section 3.3, Figure 9c). In the correlation shown in Figure 5, these influences are largely averaged out by using binned data.

3.2 Influences during the early stage of expansion of ship emission plumes

Effect of wind speed. As previously mentioned, coagulation reduces the particle number concentration more efficiently when the latter is high. This is especially the case during transport of exhaust within the exhaust system of the ships. Emission into ambient air causes a sudden dilution of the exhaust, which quickly quenches coagulation. However, even for a given particle number concentration at the location of emission, the level of further coagulation depends on the concentration level in the transported plume, which is expected to depend on the ambient wind speed, as it influences the degree of dilution in this phase of emission. In addition, lower concentration levels result in reduced condensation of vapors in the cooled exhaust gas (Hinds, 1999). Both effects can be clearly observed in our ship emission plume data as shown in Fig. 6: With increasing wind speed (stronger dilution) particle mass emission factors are reduced (less condensation) while particle number emission factors strongly increase (less coagulation). Over the range of observed ambient wind speeds from about 2 m s^{-1} up to ~12 m s^{-1} we observe a reduction of the PM_1 emissions per kg of burned fuel by about 40 %, which is similarly reflected in the EFs of condensing species like sulfate; due to the neutralization of sulfuric acid with ambient ammonia (NH_3), the ammonium EF shows the same behaviour (see Fig 6 (a)). However, there is no obvious reason why the EF for BC is also reduced at higher wind speed, indicating that, apart from condensation, another unknown effect might also play a role; potentially reduced apparent BC concentrations due to reduced co–condensed aerosol mass in the Aethalometer might explain parts of this increase. For the particle number emission factor the dilution effect is even more pronounced: Over this range of wind speeds the number of particles emitted per unit of fuel increases more than 3–fold (Fig. 6 (b)).

The effect of reduced coagulation and condensation at higher wind speed is also reflected in the observed particle size distributions: At higher wind speed the particles in the emission plume are smaller than under less windy conditions (see Fig. 6 (c)). Also the width of the particle size distribution is smaller at higher wind speed and more dominated by the combustion mode particles that, according to Petzold et al. (2008), mainly consist of BC and organic material. Note that in this study we only found apparently monomodal size distributions of particles in the ship emission plumes (see Fig. S8).

3.3 Atmospheric processes during transport of ship emission plumes

Due to the large range of observed plume ages, the ship emission plumes of the AQABA dataset contain information about the influence of atmospheric aging on plume characteristics. The investigation of atmospheric processing and aging using EFs and average excess plume concentration ratios is possible as these quantities already account for plume dilution effects. We will mainly focus on gas–to–particle conversion and associated chemical reactions in ship emission plumes during atmospheric aging.

Nitrogen oxide processing. Atmospheric processing of emitted nitrogen oxides is driven by O_3 as well as OH, HO_2 and RO_2 radicals and affects both the partitioning between NO and NO_2 and the conversion of NO_x into nitric acid and finally nitrate aerosol.

NO, the major NO_x component in ship exhaust systems (ca. 95 %) (Song et al., 2003; Williams et al., 2009), depletes ambient O_3 and is, as initial NO concentrations in the exhaust are far larger than ambient O_3 concentrations, partially converted into NO_2 rapidly after emission from the ship stack, causing NO_2 fractions in the order of the former ambient O_3 in young plumes. Song et al. (2003) modelled the dispersion and chemical evolution of ship emission plumes in the MBL with a Lagrangian plume model, based on defined background photochemical input parameters and estimates for the ship's NO_x emissions, and observed a rapid establishment of the NO_2 to NO_x ratio in ship emission plumes after O_3 titration during daylight hours. We observe~~,~~ that the NO to NO_2 ratio decreases quickly down to 0.2 (i.e. one third of ~~its initial~~the ratio measured in the youngest plume age bin) during the first half hour of atmospheric transport of ship plumes emitted during daytime. The photochemical equilibrium seems to be established when reaching this ratio and we do not find a subsequent change of it in the range of transport times covered by this study (up to 115 min, Fig. 7 (a)). The partial recovery of the ozone level over time (see Fig. S9) suggests the presence of reactive organic compounds.

Further oxidation of NO_2 in the aging plume involves hydroxyl radicals as well as ozone. Directly after exhaust release the OH radical production is strongly suppressed due to the lack of precursors (e.g. ozone) and increases (during daylight hours) in the aging plume with the recovery of O_3 and mixing of MBL air into the plume. In addition, during the first stages of plume aging, depending on local NO_x concentration and therefore on the dilution of the ship exhaust, the much more abundant HO_2 radical is converted increasingly to OH without consuming O_3 (R1) so that the OH radical concentration in the plume is enhanced (Song et al., 2003).

$$\mathbf{NO + HO_2 \longrightarrow NO_2 + HO} \qquad \text{(R1)}$$

Besides that, the concentration of N_2O_5, present essentially only at night–time, increases with increasing NO_x concentration in the ship emission plume (Song et al., 2003).

$$\mathbf{NO_2 + OH \longrightarrow HNO_3} \qquad \text{(R2)}$$

$$\mathbf{NO_2 + O_3 \longrightarrow NO_3 + O_2} \qquad \text{(R3)}$$

$$\mathbf{NO_3 + NO_2 + M \rightleftharpoons N_2O_5 + M} \qquad \text{(R4)}$$

$$\mathbf{N_2O_5 + H_2O\ (het.) \longrightarrow HNO_3} \qquad \text{(R5)}$$

These two effects cause the lifetime of NO_x in aging ship emission plumes to be shortened compared to processes in the surrounding MBL during the day (R2) and night (R3 to R5) (Chen et al., 2005; Song et al., 2003). As a consequence of these processes, NO_x is increasingly consumed as the plume ages. We found a removal of almost half of the nitrogen oxides from the emission plume within the observed range of short wavelength UV radiation exposures (potential photochemical processing; see Fig. 7 (c)); at the same time nitric acid and – depending on partitioning between gas and particle phase – nitrate–containing aerosol is produced (see Fig. S10). Regarding the NO_3^- emission factor (not differentiated between day and night–time data), most data points follow a correlation with very low increase of the apparent $EF_{NO_3^-}$, with generally very low apparent $EF_{NO_3^-}$ possibly due to the high ambient temperatures during this study, favouring the partitioning of this species into the gas phase. However, a second branch with larger slope was found that could not be explained by the available data or information (including ambient temperature, day/night differences, or measurement location).

Oxidation of SO₂. As described earlier, diesel engine systems primarily emit fuel sulfur as SO_2 so that, in principle, particulate sulfate is not formed until the release of the exhaust into the atmosphere (Pirjola et al., 2014; Moldanová et al., 2009). Following the emission into ambient air, SO_2 is oxidized by OH radicals and finally partitions into the particle phase mainly as H_2SO_4 (see Reactions (R6) to (R8); Lovejoy et al., 1996), which was concluded in previous studies from the absence of NH_4^+ and a significant fraction of sulfate–bound water in the particle phase (Petzold et al., 2008; Pokhrel and Lee, 2015; Schneider et al. 2005).

$$\mathbf{SO_2 + OH + M \longrightarrow HOSO_2 + M} \quad \text{(R6)}$$

$$\mathbf{HOSO_2 + O_2 \longrightarrow HO_2 + SO_3} \quad \text{(R7)}$$

$$\mathbf{SO_3 + H_2O \rightarrow\rightarrow H_2SO_4} \quad \text{(R8)}$$

We found the conversion of SO_2 to SO_4^{2-} to be promoted by high water vapor concentration, i.e. absolute humidity (see Fig. S11 (a)), which is consistent with Reaction (R8). Conversion of SO_2 into sulfate aerosol was observed to reduce the SO_2 to SO_4^{2-} ratio by a factor of two within the aging times covered in this study (see Fig. 7 (b)). This is accompanied by a strong increase of the sulfate EF and, due to neutralization with ammonia mixed into the plume during atmospheric dilution, by an increase of the ammonium EF. As a consequence, the PM_1 EF increases over time (see Fig. 7 (c)). The formation of secondary inorganic aerosol during plume transport therefore doubles the initial PM_1 emission from the ships within the covered range of potential photochemical processing (see next paragraph for the contribution of secondary organic aerosol). No accumulation of SO_3 or H_2SO_4 in the gas phase is expected to occur in the process as the calculated weight percentage of fuel sulfur derived from the EFs of SO_2 and SO_4^{2-} does not show a discernable dependency on the plume age (see Fig. S11 (b)), i.e. there is no indication for any “missing” sulfur.

Formation of secondary organic aerosol. Even though VOCs were measured during the AQABA field campaign, they were not included in the investigation of ship emission plumes because the (potential) ship emission events were not reflected in the corresponding VOC time series. Moreover, unlike the mass of particulate inorganic species in the plume aerosol the mass of particulate organics does not increase significantly during photochemical aging (see Fig. S12). The same is true for the O/C ratio, which also does not show a clear sign of aging of organic material within the observed range of short wavelength UV radiation exposure (see Fig. 8 (a)). However, the particulate organic EF and the O/C ratio show a positive correlation (see Fig. 8 (b)), generally suggesting an increase of organic particulate mass, potentially through oxidation of gas phase organic material during plume transport.

Development of aerosol composition and neutralization of inorganic acids. As discussed in the sections above, the chemical composition of aerosol particles in ship emission plumes depends on various factors. Combustion conditions mainly influence BC emissions, fuel quality (with sulfur content affecting the consumption of lubricating agent) has an effect on organic aerosol components in the plume and atmospheric processes mainly generate additional secondary inorganic aerosol components, which also partially depend on fuel sulfur content. To investigate the changes in chemical composition of the plume aerosol particles we calculated ~~average~~ typical particle compositions for three different plume age intervals including approximately the same number of data points, using the medians of the respective emission factors: for plumes younger than 16 min, for plume ages between 16 and 40 min, and for plumes older than 40 min (see Fig. 9 (d)). The processes during plume aging are reflected in these ~~average~~ relative compositions: The organic fraction contributes increasingly less and the inorganic fraction increasingly more to the particle phase. This is due to strong increases in the inorganic emission factors during plume transport, while the organic EF increases only very slightly. When looking separately at the plume development during day and night time, we find these effects to be much stronger during the day, compared to the night (see Figure S14), consistent with photochemical processes contributing to the formation of secondary inorganic aerosol components. We emphasise that ~~the higher average fraction of BC in PM_1 from plumes older than 40 min is not an effect of atmospheric aging but likely due to slight differences in combustion efficiency~~the relatively low number of data points for some species during individual plume age intervals and large scatter of emission factors due to other influences results in some of the variability observed in the relative composition of the particle phase. ~~Regardless, BC remains constant within the margins of error.~~ As shown in Fig. 7 (c), the photochemical formation of particulate sulfuric acid is accompanied by an increase in particulate ammonium due to (partial) neutralization of sulfuric and nitric acid, associated with the formation of particulate ammonium (bi)sulfate and ammonium nitrate. This is a consequence of ammonia being mixed into the diluting plume from the marine background air. If we take into account that 3 eq. of NH_3 neutralize 1 eq. H_2SO_4 and 1 eq. HNO_3 in the particle phase, the average degree of neutralization increases from 61 % for plumes younger than 16 min to 69 % for plumes between 16 and 40 min of age up to 95 % for plumes older than 40 min.

Other trace gases: formation and degradation of HCHO. Formaldehyde (HCHO) has previously been observed in ship emission plumes and was explained by enhanced photochemical formation from background CH_4 (Lowe and Schmidt, 1983) due to higher OH concentrations in the plume, from VOC oxidation (Marbach et al., 2009), or with direct emission from the ships due to incomplete combustion (Williams et al., 2009). Our observations show that the apparent HCHO emission factors increase along with photochemical aging of the plume (see Fig. 10), in agreement with photochemical formation processes. The regression intercept (i.e. EF for negligible potential photochemical plume processing), however, is not significantly different from zero HCHO emissions and therefore does not suggest direct emissions of HCHO by the ships (see Table 2). Atmospheric decomposition of HCHO in the troposphere (R9 to R12) occurs within a few hours under daylight conditions and leads to the formation of CO in the aging plume (Lowe and Schmidt, 1983).

$$\mathbf{HCHO} + h\nu \longrightarrow \mathbf{CO} + \mathbf{H_2} \qquad \text{(R9)}$$

$$\mathbf{HCHO} + h\nu \longrightarrow \mathbf{HCO} + \mathbf{H} \qquad \text{(R10)}$$

$$\mathbf{HCHO + OH \longrightarrow HCO + H_2O} \tag{R11}$$

$$\mathbf{HCO + O_2 \longrightarrow CO + HO_2} \tag{R12}$$

As a consequence of these processes, we observe an increase of the apparent CO emission factor in the photochemically aging plume (see Fig. 10) which results in apparently 2–4 times higher apparent CO emission factors in the aged plume, compared to the actual emissions from the ship stacks due to incomplete combustion of the fuel. The direct CO emissions from the ships can therefore only be determined from aged plumes by accounting for this CO increase during plume aging (see correlation function in Table 2).

Development of particle size and number concentration in the aging plume. As discussed above, the particle mass in the ship plumes increases mainly due to the formation of $(NH_4)_2SO_4$ during atmospheric aging and the mass of particulate organics increases slightly through oxidation. In addition, coagulation of particles in the plume should result in fewer but larger particles. However, we observe neither a growth of particles nor an increase in the width of the size distribution with increasing plume age (see Fig. 9 (a) and (b)). A reason for this might be that for spherical particles the particle diameter scales only with the third root of the particle mass and therefore the resulting small increase of particle size might not be observable within the large variability due to other influencing factors. Another explanation could be that especially soot particles in freshly emitted diesel exhaust usually show an irregular shape with a fractal dimension well below three, which may collapse when vapor condenses onto the particles forming less fractal and more compact (more spherical) particles. This effect causes an increase of the particle mass without resulting in an equivalent increase of the measured particle size (*here*: mobility diameter; Pagels et al. 2009).

As illustrated in Fig. 9 (c), we do not observe a dependence of the particle number EF on the plume age during daylight hours, whereas a decrease is observed for ship emission plumes that were detected during night–time. In general, there are mainly two opposite effects that change the particle number concentration in an expanding plume over time (dilution excluded), coagulation and new particle formation. While the particle number concentration decrease during night–time transport could be due to coagulation within the plume. This effect could be outbalanced or at least superimposed by new particle formation during daytime. However, the large scatter in the daytime particle number EF shows that there are strong additional factors influencing this plume property and detailed microphysical modeling studies are needed to disentangle the different processes and elucidate their relative importance.

3.4 Average ship emission plume quantities and comparison with literature data

For comparison with data available in the literature, we calculated average emission factors, particle size distribution data and ratios of plume components for all ship emission plumes of the AQABA dataset (Table 3). Diesch et al. (2013), Lack et al. (2009) and Williams et al. (2009) as well as Jonsson et al. (2011) report the results of studies conducted in ECAs that include a large sample of measured ship emission plumes (> 100), whereas Petzold et al. (2008) (in ECA), Sinha et al. (2003) (not in

ECA), and Juwono et al. (2013) (not in ECA) investigated individual ship emission plumes of a small number of ships (one or two) under various operating conditions.

In general, the average apparent particle mass emission factors (both for total PM and for individual species) from this study are significantly higher (ca. factor 1.5 to 4) than those previously reported in the literature, which is primarily due to the fact that the AQABA field campaign did not take place in an ECA and that a significant number of atmospherically aged and processed ship emission plumes with thus higher particle mass concentrations (see Sect. 3.3) were analyzed. Therefore, particle mass emission factors that are inferred for the time of emission (fitting parameters a in Table 2) are lower than average apparent EFs and thus closer to (but still somewhat above) listed literature data. The average BC emission factor determined for the identified ship emission plumes of the AQABA dataset is in good agreement with the data given by Lack et al. (2009). Buffaloe et al. (2014, not included in Table 3) focused on the investigation of BC in 135 individual emission plumes of 71 different ships operating off the Californian coast (an ECA) and report a lower average BC emission factor of (0.31 ± 0.31) g (kg fuel)$^{-1}$, though still higher than EF_{BC} derived from other studies (Table 3) which are more in the range of 0.2 g (kg fuel)$^{-1}$. As we have shown (Sect. 3.1, Fig. 3), EF_{BC} strongly depends on the gross tonnage of the emitting vessel, with the lowest EF_{BC} found for a gross tonnage of ~50 000 with ~0.25 g (kg fuel)$^{-1}$, which is closer to the range observed in previous studies. Therefore, the observed differences could be due to different fleet compositions in the various studies, although other influences like different average ship speeds (compare Fig. 3 (b)) are also likely to play a role. Unlike the average particle mass emission factors, the average particle number emission factor from our study is consistent with the listed literature data. As particle coagulation is mainly relevant during the early stage of plume expansion, when the local PNC is high, plume aging on the considered time scale is not a strongly influencing factor for the particle number (PN) emission factor.

As EFs of many trace–gases mainly depend on vessel characteristics and fuel quality, data available in the literature can vary significantly. Sinha et al. (2003) conducted a study off the Namibian coast and for a tanker that was assumed to burn MDO (0.1 wt. % fuel S) they report an SO_2 emission factor of (2.9 ± 0.2) g (kg fuel)$^{-1}$ and for a container vessel that was assumed to burn HFO (2.4 wt. % fuel S) an SO_2 emission factor of (52.2 ± 3.7) g (kg fuel)$^{-1}$. The average SO_2 emission factor ((26 ± 6) g (kg fuel)$^{-1}$) and the average weight percentage of fuel sulfur (1.4 wt. % fuel S) of our study are in good agreement with the averaged data of both vessels from their measurements as our study covers a broad range of fuel sulfur contents. The same statement as for the particle mass emission factors regarding higher values due to plume aging is true for the average apparent HCHO and CO emission factors as the analysis shows that these species were also formed during the aging of the ship emission plumes. The average modified combustion efficiency presented in Table 3 was determined by using the CO emission factors that were referred to the time of emission via the slope of the linear correlation (Table 2) and calculating the average of these values, while for all other values in this table the actually observed concentrations were used.

4 Summary and conclusions

A variety of gas and particle phase species in 252 ship emission plumes measured in the Mediterranean Sea and around the Arabian Peninsula during the two–month shipborne AQABA field campaign in summer 2017 were investigated. For this purpose, a method based on commercially available historical AIS records that include ship position, course and velocity was developed and applied to identify the ship emission plumes and characterize them with respect to their source and age by reconstructing the intersection point of the source vessel track and the track of measured air masses. Observed ship emission plumes were up to 115 min old and transported up to 38 km. Based on the time dependent exponential decay of the average excess plume concentration of the chemically inert CO_2 in ship emission plumes a dispersion lifetime of (70 ± 15) min and a dilution down to a level indistinguishable from background within (260 ± 60) min were determined. Emission factors (EFs) of the particle number and of particle and gas phase species masses in ship emission plumes were calculated as quantities that account for plume dilution and refer to the amount of burned fuel. These EFs were used to investigate the influences on the emission plume characteristics caused by ship parameters and the combustion process as well as by atmospheric effects during the early stage of exhaust release and during plume aging in order to address the following scientific questions. Figure 11 gives an overview of the observed processes and how they affect plume characteristics.

How does e.g. the ship velocity affect the combustion efficiency? We observed more efficient fuel combustion at higher ambient pressure–to–temperature ratios (i.e. higher O_2–to–fuel mixing ratios in the combustion chamber) and for ships with higher velocities as well as for vessels with medium size gross tonnages. This was reflected in the BC emission factor being lower and was accompanied by larger NO_x emission factors. Additionally, it was found that more efficient fuel combustion causes a ~~lower~~ higher initial ratio of NO to NO_2. (see Fig. 3 and Fig. S13)

How does the fuel sulfur content influence the quantity of emitted species? We found that larger vessels, that typically burn lower grade fuel, emit more SO_2 and, due to the higher consumption of lubricating oil as a corrosion preventive, more organic aerosol and thus promote the formation of more PM during atmospheric processing of the corresponding emission plumes. (see Fig. 4)

What are the effects of the exhaust system's size and thus of the exhaust's residence time within the pipes? It was shown that larger vessels emit less particles by number per kg of burned fuel, likely due to their longer exhaust system that favors particle coagulation before the coagulation process is quenched when the exhaust is released into ambient air. (see Fig. 5)

How do atmospheric dilution, transport, and aging affect the characteristics of ship emission plumes? We observed that ambient wind speed, which affects the dilution of the emission plume at the ship stack exit, significantly influences the particle number concentration (PNC): A lower wind speed results in less diluted plumes and thus promotes particle coagulation as well as vapor condensation and as a consequence causes a lower PNC EF accompanied by larger particles and a higher particle mass EF. Furthermore, due to the long plume aging intervals covered in this study, we were able to observe and quantify atmospheric reactions and processes like O_3 reduction and recovery accompanied by the conversion between NO and NO_2, the photochemical formation of HCHO and CO, the formation of secondary aerosol, namely the oxidation of NO_x to NO_3^- and of

SO_2 to SO_4^{2-}, and the neutralization of acids in the particle phase through the uptake of NH_3 from ambient air. It was shown that the organic fraction which we mainly trace back to lubricating oil from the ship engine system contributes increasingly less and the inorganic fraction increasingly more to the particle phase with plume aging, although higher O/C ratios were found for higher particulate organic EFs indicating the increase of particulate organics mass through atmospheric oxidation. (see Figs. 6 to 9)

From this study, the wind velocity was identified as the strongest factor influencing the PN emission factor as well as the median diameter and width of the particle number size distribution. Particulate organics and SO_2 emission factors were mainly influenced by fuel sulfur content, strongly associated with vessel gross tonnage. The largest influence on the apparent EFs of inorganic particle phase species (except BC), the PM_1, as well as the apparent CO and HCHO emission factors was found to be atmospheric aging. Finally, the ship velocity was identified to dominate the BC and NO_x emission factors.
The quantification of observed influences on or processes in ship emission plumes by parameterization will help to refine models in this research field. However, detailed numerical simulation studies are required to describe the relevant microphysical and chemical processes quantitatively.

Data availability

The data used in this study are archived and distributed through the KEEPER service of the Max Planck Digital Library (https://keeper.mpdl.mpg.de) and will be available from August 2019 to all scientists agreeing to the AQABA protocol.

Author contributions

SC performed the analysis of ship emission plumes during the AQABA field campaign and wrote the manuscript. FD supervised this study. Aerosol particle measurements and data were provided by FD, FF, JB, ED, SB, and HC. JP contributed CO and CO_2 measurments and data. O_3, SO_2, and NO_x measurments and data were provided by PE, NF, and JC and JO^1D values were measured by JS. IT, DD, BH, and HF provided NO, NO_2, and HCHO measurements and data. HH took responsibility for the scientific coordination of the field campaign on–board the research vessel. All authors contributed to data interpretation and manuscript revision and approved the submitted version.

Competing interests

The authors declare that they have no conflict of interest.

Acknowledgements

The authors are grateful to T. Böttger, P. Schumann, C. Koeppel, and M. Dorf for technical support in the preparation and conduction of the AQABA field campaign. They thank U. Parchatka for supporting the NO and NO_2 measurements during the field campaign. M. Anfield from MarineTraffic is acknowledged for fruitful support in the identification of AIS data. The Max Planck Society covered the majority of the costs for the field campaign; University of Manchester is acknowledged for financial support for data analysis.

References

Agrawal, H., Malloy, Q. G. J., Welch, W. A., Wayne Miller, J., and Cocker, D. R.: In–use gaseous and particulate matter emissions from a modern ocean going container vessel, Atmos. Environ., 42, 5504–5510, https://doi.org/10.1016/j.atmosenv.2008.02.053, 2008.

Aiken, A. C., DeCarlo, P. F., Kroll, J. H., Worsnop, D. R., Huffman, J. A., Docherty, K. S., Ulbrich, I. M., Mohr, C., Kimmel, J. R., Sueper, D., Sun, Y., Zhang, Q., Trimborn, A., Northway, M., Ziemann, P. J., Canagaratna, M. R., Onasch, T. B., Alfarra, M. R., Prevot, A. S. H., Dommen, J., Duplissy, J., Metzger, A., Baltensperger, U., and Jimenez, J. L.: O/C and OM/OC Ratios of Primary, Secondary, and Ambient Organic Aerosols with High–Resolution Time–of–Flight Aerosol Mass Spectrometry, Environ. Sci. Technol., 42, 4478–4485, https://doi.org/10.1021/es703009q, 2008.

Alföldy, B., Lööv, J. B., Lagler, F., Mellqvist, J., Berg, N., Beecken, J., Weststrate, H., Duyzer, J., Bencs, L., Horemans, B., Cavalli, F., Putaud, J.–P., Janssens–Maenhout, G., Csordás, A. P., van Grieken, R., Borowiak, A., and Hjorth, J.: Measurements of air pollution emission factors for marine transportation in SECA, Atmos. Meas. Tech., 6, 1777–1791, https://doi.org/10.5194/amt-6-1777-2013, 2013.

Bermudez, V., Serrano, J. R., Piqueras, P., Gomez, J., Bender, S.: Analysis of the role of altitude on diesel engine performance and emissions using an atmosphere simulator, International Journal of Engine Research 18, 105-117, DOI:10.1177/1468087416679569, 2017.

Buffaloe, G. M., Lack, D. A., Williams, E. J., Coffman, D., Hayden, K. L., Lerner, B. M., Li, S.–M., Nuaaman, I., Massoli, P., Onasch, T. B., Quinn, P. K., and Cappa, C. D.: Black carbon emissions from in–use ships: a California regional assessment, Atmos. Chem. Phys., 14, 1881–1896, https://doi.org/10.5194/acp-14-1881-2014, 2014.

Cappa, C. D., Williams, E. J., Lack, D. A., Buffaloe, G. M., Coffman, D., Hayden, K. L., Herndon, S. C., Lerner, B. M., Li, S.–M., Massoli, P., McLaren, R., Nuaaman, I., Onasch, T. B., and Quinn, P. K.: A case study into the measurement of ship emissions from plume intercepts of the NOAA ship Miller Freeman, Atmos. Chem. Phys., 14, 1337–1352, https://doi.org/10.5194/acp-14-1337-2014, 2014.

Chang, Y., Mendrea, B., Sterniak, J., Bohac, S. V.: Effect of Ambient Temperature and Humidity on Combustion and Emissions of a Spark-Assisted Compression Ignition Engine, J. Eng. Gas Turbines Power, 139, 51501-1 – 51501-7, https://doi.org/10.1115/1.4034966, 2017.

Chen, D., Zhao, N., Lang, J., Zhou, Y., Wang, X., Li, Y., Zhao, Y., and Guo, X.: Contribution of ship emissions to the concentration of $PM_{2.5}$: A comprehensive study using AIS data and WRF/Chem model in Bohai Rim Region, China, Sci. Total Environ., 611, 1476–1486, https://doi.org/10.1016/j.scitotenv.2017.07.255, 2018.

Chen, G., Huey, L. G., Trainer, M., Nicks, D., Corbett, J., Ryerson, T., Parrish, D., Neuman, J. A., Nowak, J., Tanner, D., Holloway, J., Brock, C., Crawford, J., Olson, J. R., Sullivan, A., Weber, R., Schauffler, S., Donnelly, S., Atlas, E., Roberts, J., Flocke, F., Hübler, G., and Fehsenfeld, F.: An investigation of the chemistry of ship emission plumes during ITCT 2002, J. Geophys. Res., 110, 1–15, https://doi.org/10.1029/2004JD005236, 2005.

Chu–Van, T., Ristovski, Z., Pourkhesalian, A. M., Rainey, T., Garaniya, V., Abbassi, R., Jahangiri, S., Enshaei, H., Kam, U.–S., Kimball, R., Kimball, R., Yang, L., Zare, A., Bartlett, H., and Brown, R. J.: On–board measurements of particle and gaseous emissions from a large cargo vessel at different operating conditions, Environ. Pollut., 237, 832–841, https://doi.org/10.1016/j.envpol.2017.11.008, 2018.

Corbett, J. J., Fischbeck, P. S., and Pandis, S. N.: Global nitrogen and sulfur inventories for oceangoing ships, J. Geophys. Res., 104, 3457–3470, https://doi.org/10.1029/1998JD100040, 1999.

Corbett, J. J., Winebrake, J. J., Green, E. H., Kasibhatla, P., Eyring, V., and Lauer, A.: Mortality from Ship Emissions: A Global Assessment, Environ. Sci. Technol., 41, 8512–8518, https://doi.org/10.1021/es071686z, 2007.

DeCarlo, P. F., Kimmel, J. R., Trimborn, A., Northway, M. J., Jayne, J. T., Aiken, A. C., Gonin, M., Fuhrer, K., Horvath, T., Docherty, K. S., Worsnop, D. R., and Jimenez, J. L.: Field–deployable, high–resolution, time–of–flight aerosol mass spectrometer, Anal. Chem., 78, 8281–8289, https://doi.org/10.1021/ac061249n, 2006.

Diesch, J.–M., Drewnick, F., Klimach, T., and Borrmann, S.: Investigation of gaseous and particulate emissions from various marine vessel types measured on the banks of the Elbe in Northern Germany, Atmos. Chem. Phys., 13, 3603–3618, https://doi.org/10.5194/acp-13-3603-2013, 2013.

Drewnick, F., Böttger, T., von der Weiden–Reinmüller, S.–L., Zorn, S. R., Klimach, T., Schneider, J., and Borrmann, S.: Design of a mobile aerosol research laboratory and data processing tools for effective stationary and mobile field measurements, Atmos. Meas. Tech., 5, 1443–1457, https://doi.org/10.5194/amt-5-1443-2012, 2012.

Drinovec, L., Močnik, G., Zotter, P., Prévôt, A. S. H., Ruckstuhl, C., Coz, E., Rupakheti, M., Sciare, J., Müller, T., Wiedensohler, A., and Hansen, A. D. A.: The "dual–spot" Aethalometer: an improved measurement of aerosol black carbon with real–time loading compensation, Atmos. Meas. Tech., 8, 1965–1979, https://doi.org/10.5194/amt-8-1965-2015, 2015.

Eger, P. G., Helleis, F., Schuster, G., Phillips, G. J., Lelieveld, J., and Crowley, J. N.: Chemical ionization quadrupole mass spectrometer with an electrical discharge ion source for atmospheric trace gas measurement, Atmos. Meas. Tech., 12, 1935–1954, https://doi.org/10.5194/amt-12-1935-2019, 2019.

Equasis: http://www.equasis.org/EquasisWeb/public/HomePage, last access: 29 March 2019.

FleetMon: https://www.fleetmon.com/, last access: 29 March 2019.

Fridell, E., Steen, E., and Peterson, K.: Primary particles in ship emissions, Atmos. Environ., 42, 1160–1168, https://doi.org/10.1016/j.atmosenv.2007.10.042, 2008.

Hinds, W. C.: Aerosol Technology: Properties, Behavior, and Measurement of Airborne Particles, Wiley–Interscience: New York, 1999.

IMO: http://www.imo.org/en/Pages/Default.aspx, last access: 12 March 2019.

Jonsson, Å. M., Westerlund, J., and Hallquist, M.: Size–resolved particle emission factors for individual ships, Geophys. Res. Lett., 38, 1–5, https://doi.org/10.1029/2011GL047672, 2011.

Juwono, A. M., Johnson, G. R., Mazaheri, M., Morawska, L., Roux, F., and Kitchen, B.: Investigation of the airborne submicrometer particles emitted by dredging vessels using a plume capture method, Atmos. Environ., 73, 112–123, https://doi.org/10.1016/j.atmosenv.2013.03.024, 2013.

Khalid, A.: Effect of Ambient Temperature and Oxygen Concentration on Ignition and Combustion Process of Diesel Spray, Asian J. Sci. Res., 6, 434–444, https://doi.org/10.3923/ajsr.2013.434.444, 2013.

Kim, H. S., Song, C. H., Park, R. S., Huey, G., and Ryu, J. Y.: Investigation of ship–plume chemistry using a newly–developed photochemical/dynamic ship–plume model, Atmos. Chem. Phys., 9, 7531–7550, https://doi.org/10.5194/acp-9-7531-2009, 2009.

Lack, D. A., Corbett, J. J., Onasch, T., Lerner, B., Massoli, P., Quinn, P. K., Bates, T. S., Covert, D. S., Coffman, D., Sierau, B., Herndon, S., Allan, J., Baynard, T., Lovejoy, E., Ravishankara, A. R., and Williams, E.: Particulate emissions from commercial shipping: Chemical, physical, and optical properties, J. Geophys. Res., 114, 1–16, https://doi.org/10.1029/2008JD011300, 2009.

Levin, M., Gudmundsson, A., Pagels, J. H., Fierz, M., Mølhave, K., Löndahl, J., Jensen, K. A., and Koponen, I. K.: Limitations in the Use of Unipolar Charging for Electrical Mobility Sizing Instruments: A Study of the Fast Mobility Particle Sizer, 49, 556–565, https://doi.org/10.1080/02786826.2015.1052039, 2015.

Lovejoy, E. R., Hanson, D. R., and Huey, L. G.: Kinetics and Products of the Gas–Phase Reaction of SO_3 with Water, J. Phys. Chem., 100, 19911–19916, https://doi.org/10.1021/jp962414d, 1996.

Lowe, D. C., and Schmidt, U.: Formaldehyde (HCHO) measurements in the nonurban atmosphere, J. Geophys. Res., 88, 10844–10858, https://doi.org/10.1029/JC088iC15p10844, 1983.

Marbach, T., Beirle, S., Platt, U., Hoor, P., Wittrock, F., Richter, A., Vrekoussis, M., Grzegorski, M., Burrows, J. P., and Wagner, T.: Satellite measurements of formaldehyde linked to shipping emissions, Atmos. Chem. Phys., 9, 8223–8234, https://doi.org/10.5194/acp-9-8223-2009, 2009.

Mardia, K. V., and Jupp, P. E.: Directional statistics, Wiley, Chichester, UK, 2000.

MarineTraffic: https://www.marinetraffic.com/, last access: 26 March 2019.

Metz, B., Davidson, O. R., Bosch, P. R., Dave, R., and Meyer, L. A. (Eds): Climate Change 2007: Mitigation, Contribution of Working Group III to the Fourth Assessment Report of the Intergovernmental Panel on Climate Change, IPCC, Cambridge University Press, Cambridge, United Kingdom and New York, NY, USA., 325 pp, 2007.

Meusel, H., Kuhn, U., Reiffs, A., Mallik, C., Harder, H., Martinez, M., Schuladen, J., Bohn, B., Parchatka, U., Crowley, J. N., Fischer, H., Tomsche, L., Novelli, A., Hoffmann, T., Janssen, R. H. H., Hartogensis, O., Pikridas, M., Vrekoussis, M., Bourtsoukidis, E., Weber, B., Lelieveld, J., Williams, J., Pöschl, U., Cheng, Y., and Su, H.: Daytime formation of nitrous acid at a coastal remote site in Cyprus indicating a common ground source of atmospheric HONO and NO, Atmos. Chem. Phys., 16, 14475–14493, https://doi.org/10.5194/acp-16-14475-2016, 2016.

Mohd Noor, C. W., Noor, M. M., and Mamat, R.: Biodiesel as alternative fuel for marine diesel engine applications: A review, Renew. Sust. Energ. Rev., 94, 127–142, https://doi.org/10.1016/j.rser.2018.05.031, 2018.

Moldanová, J., Fridell, E., Popovicheva, O., Demirdjian, B., Tishkova, V., Faccinetto, A., and Focsa, C.: Characterisation of particulate matter and gaseous emissions from a large ship diesel engine, Atmos. Environ., 43, 2632–2641, https://doi.org/10.1016/j.atmosenv.2009.02.008, 2009.

Moldanová, J., Fridell, E., Winnes, H., Holmin–Fridell, S., Boman, J., Jedynska, A., Tishkova, V., Demirdjian, B., Joulie, S., Bladt, H., Ivleva, N. P., and Niessner, R.: Physical and chemical characterisation of PM emissions from two ships operating in European Emission Control Areas, Atmos. Meas. Tech., 6, 3577–3596, https://doi.org/10.5194/amt-6-3577-2013, 2013.

Nash, T.: The colorimetric estimation of formaldehyde by means of the Hantzsch reaction, Biochem. J., 55, 416–421, https://doi.org/10.1042/bj0550416, 1953.

Nunes, R. A. O., Alvim–Ferraz, M. C. M., Martins, F. G., and Sousa, S. I. V.: Assessment of shipping emissions on four ports of Portugal, Environ. Pollut., 231, 1370–1379, https://doi.org/10.1016/j.envpol.2017.08.112, 2017.

Pagels, J., Khalizov, A. F., McMurry, P. H., and Zhang R. Y.: Processing of Soot by Controlled Sulphuric Acid and Water Condensation – Mass and Mobility Relationship, Aerosol Sci. Tech., 43, 629–640, https://doi.org/10.1080/02786820902810685, 2009.

Petzold, A., Hasselbach, J., Lauer, P., Baumann, R., Franke, K., Gurk, C., Schlager, H., and Weingartner, E.: Experimental studies on particle emissions from cruising ship, their characteristic properties, transformation and atmospheric lifetime in the marine boundary layer, Atmos. Chem. Phys., 8, 2387–2403, https://doi.org/10.5194/acp-8-2387-2008, 2008.

Pirjola, L., Pajunoja, A., Walden, J., Jalkanen, J.–P., Rönkkö, T., Kousa, A., and Koskentalo, T.: Mobile measurements of ship emissions in two harbour areas in Finland, Atmos. Meas. Tech., 7, 149–161, https://doi.org/10.5194/amt-7-149-2014, 2014.

Pokhrel, R., and Lee, H.: Estimation of air pollution from the OGVs and its dispersion in a coastal area, Ocean Eng., 101, 275–284, https://doi.org/10.1016/j.oceaneng.2015.04.023, 2015.

Rajewski, A.: Evaluating internal combustion engine's performance, Wärtsilä Technical Journal 2/2018, 18-23, 2018.

Rößler, M., Koch, T., Janzer, C., and Olzmann, M.: Mechanisms of the NO_2 Formation in Diesel Engines, MTZ Worldw., 78, 70–75, https://doi.org/10.1007/s38313-017-0057-2, 2017.

Schneider, J., Hock, N., Weimer, S., and Borrmann, S.: Nucleation Particles in Diesel Exhaust: Composition Inferred from In Situ Mass Spectrometric Analysis, Environ. Sci. Technol., 39, 6153–6161, https://doi.org/10.1021/es049427m, 2007.

Sinha, P., Hobbs, P. V., Yokelson, R. J., Christian, T. J., Kirchstetter, T. W., and Bruintjes, R.: Emissions of trace gases and particles from two ships in the southern Atlantic Ocean, Atmos. Environ., 37, 2139–2148, https://doi.org/10.1016/S1352-2310(03)00080-3, 2003.

Smith, T. W. P., Jalkanen, J. P., Anderson, B. A., Corbett, J. J., Faber, J., Hanayama, S., O'Keeffe, E., Parker, S., Johansson, L., Aldous, L., Raucci, C., Traut, M., Ettinger, S., Nelissen, D., Lee, D. S., Ng, S., Agrawal, A., Winebrake, J. J., Hoen, M., Chesworth, S., and Pandey, A.: Third IMO Greenhouse Gas Study 2014, International Maritime Organization, London, UK, 2015.

Song, C. H., Chen, G., Hanna, S. R., Crawford, J., and Davis, D. D.: Dispersion and chemical evolution of ship plumes in the marine boundary layer: Investigation of $O_3/NO_y/HO_x$ chemistry, J. Geophys. Res., 108, 1–18, https://doi.org/10.1029/2002JD002216, 2003.

Thieser, J., Schuster, G., Schuladen, J., Phillips, G. J., Reiffs, A., Parchatka, U., Pöhler, D., Lelieveld, J., and Crowley, J. N.: A two–channel thermal dissociation cavity ring–down spectrometer for the detection of ambient NO_2, RO_2NO_2 and $RONO_2$, Atmos. Meas. Tech., 9, 553–576, https://doi.org/10.5194/amt-9-553-2016, 2016.

Tseng, W.–K., and Chang, W.–J.: Analogues between 2D Linear Equations and Great Circle Sailing, J. Navigation, 67, 101–112, https://doi.org/10.1017/S0373463313000532, 2014.

UNCTAD: https://unctadstat.unctad.org/wds/TableViewer/tableView.aspx?ReportId=93, last access: 30 March 2019.

Veness, C.: Movable Type Scripts: Calculate distance, bearing and more between Latitude/Longitude points, Movable Type Ltd, https://www.movable-type.co.uk/scripts/latlong.html, 2019.

Ward, D. E., and Radke, L. F.: Emissions measurements from vegetation fires: A comparative evaluation of methods and results, in: Fire in the Environment: The Ecological, Atmospheric, and Climatic Importance of Vegetation Fires, edited by: Crutzen, P. J., and Goldammer, J. G., Environmental Sciences Research Report 13, Wiley, Chichester, 53–76, 1993.

von der Weiden, S.–L., Drewnick, F., and Borrmann, S.: Particle Loss Calculator – a new software tool for the assessment of the performance of aerosol inlet systems, Atmos. Meas. Tech., 2, 479–494, https://doi.org/10.5194/amt-2-479-2009, 2009.

Williams, E. J., Lerner, B. M., Murphy, P. C., Herndon, S. C., and Zahniser, M. S.: Emissions of NO_x, SO_2, CO, and HCHO from commercial marine shipping during Texas Air Quality Study (TexAQS) 2006, J. Geophys. Res., 114, 1–14, https://doi.org/10.1029/2009JD012094, 2009.

Table 1: Overview of quantities measured during the AQABA field campaign that were used in this study, along with the respective measurement instruments, size ranges with the corresponding particle losses, and time resolutions. The given particle transport losses (estimated using the Particle Loss Calculator, von der Weiden~~,~~ et al., 2009) represent upper limits, as particle losses within the size ranges are lower than at its boundaries. Acronyms are introduced in Sect. 2.2.

	variable	measurement instrument	size range (particle losses)	time resolution
particle phase	PNC	CPC, TSI Model 3787 & FMPS, TSI Model 3091	5 nm (20 %) to 1 µm (10 %) & 6 nm (11 %) to 560 nm (0.2 %) [a]	10 s
	PN size distribution	FMPS, TSI Model 3091	6 nm (11 %) to 560 nm (0.2 %) [a]	10 s
	$[\mathrm{PM}_1]$ [b]	– “ –	– “ –	10 s
	[BC]	Aethalometer, Magee Scientific Model AE33	10 nm (11 %) to 1 µm (3 %)	10 s
	[PAH]	PAH monitor, EcoChem Analytics Model PAS 2000	10 nm (11 %) to 1 µm (3 %)	10 s
	$[\mathrm{SO}_4^{2-}]$, $[\mathrm{NO}_3^-]$, $[\mathrm{NH}_4^+]$ $[\mathrm{Cl}^-]$, [organics], O/C, H/C	HR–ToF–AMS, Aerodyne Research, Inc.	40 nm (9 %) to 600 nm (1 %) [c]	30 s
gas phase	[CO], $[\mathrm{CO}_2]$	CRDS, Picarro, Inc. Model G2401	N/A	1 s
	$[\mathrm{SO}_2]$	Iodide CI–QMS	N/A	10 s
	$[\mathrm{O}_3]$	Ozone monitor, 2B Technologies Model 202	N/A	10 s
	[NO], $[\mathrm{NO}_2]$	Two–Channel CLD, ECO Physics Model CLD 790 SR [d]	N/A	5 s, 1 min
	$[\mathrm{NO}_x]$	Two–Channel TD–CRDS	N/A	5 s
	[HCHO]	Formaldehyde monitor, Aero–Laser Model 4021	N/A	3 s [e]
auxiliary data	longitude, latitude	automatic weather station with GPS, Neptune, Sterela Meteo	N/A	1 s
	wind speed and direction, T, p, RH		N/A	1 s
	$J\mathrm{O}^1\mathrm{D}$ [f]	CCD spectral radio–meter, Metcon Model 85237	N/A	1 min

---

[a] Mobility and [c] vacuum aerodynamic diameter.

[b] PM_1 covers only particles with diameters $\lesssim$ 350 nm, as larger particles were not observed in the ship emission plumes.

[d] Modified version of the commercially available instrument.

[e] Effective time resolution is 170 s.

[f] The photolysis rate was calculated using wavelength resolved actinic flux data measured by the spectral radiometer.

Table 2: Correlations and corresponding fit parameters and correlation coefficients (Pearson's *R*) referring to dependencies in ship emission plumes presented in Figs. 3 to 10. *N*: number of available raw (not binned) data points.

	correlation			**fit parameters and correlation coefficient**			
	$f(x) = a + bx$	unit for $f(x)$	unit for x	a	b	R	N
ship parameters and combustion process	$EF_{BC}(p \cdot T^{-1})$	g (kg fuel)$^{-1}$	hPa·K^{-1}	29	–8.5	0.37	62
	$EF_{NO_x}(p \cdot T^{-1})$	g (kg fuel)$^{-1}$	hPa·K^{-1}	-630	210	0.28	139
	$EF_{BC}(H_2O)$	g (kg fuel)$^{-1}$	g m^{-3}	-0.16	0.05	0.15	61
	$EF_{NO_x}(H_2O)$	g (kg fuel)$^{-1}$	g m^{-3}	91	-1.7	0.24	132
	$EF_{BC}(v_{ship})$	g (kg fuel)$^{-1}$	m s^{-1}	1.5	–0.11	0.41	63
	$EF_{NO_x}(v_{ship})$	g (kg fuel)$^{-1}$	m s^{-1}	26	3.9	0.33	140
	$[NO]/[NO_2]_{obs}(v_{ship})$	–	m s^{-1}	0.076	0.032	0.18	157
	$[NO]/[NO_2]_{ini}(v_{ship})$	–	m s^{-1}	0.179	0.032	0.34	157
	wt. % fuel S(GT)	%	–	1.3	$2.1\cdot10^{-6}$	0.16	112
	$EF_{organics}$(wt. % fuel S)	g (kg fuel)$^{-1}$	%	2.1	0.95	0.21	111
	EF_{PM_1}(wt. % fuel S)	g (kg fuel)$^{-1}$	%	4.4	2.5	0.25	99
	EF_{PN}(GT)	# (kg fuel)$^{-1}$	–	$1.3\cdot10^{16}$	$–2.3\cdot10^{10}$	0.12	247
atmospheric processes early stage	$EF_{PN}(v_{wind})$	# (kg fuel)$^{-1}$	m s^{-1}	$4.5\cdot10^{15}$	$1.4\cdot10^{15}$	0.38	252
	$EF_{PM_1}(v_{wind})$	g (kg fuel)$^{-1}$	m s^{-1}	9.8	–0.35	0.15	156
	$EF_{SO_4^{2-}}(v_{wind})$	g (kg fuel)$^{-1}$	m s^{-1}	4.9	–0.25	0.23	165
	$EF_{NH_4^+}(v_{wind})$	g (kg fuel)$^{-1}$	m s^{-1}	1.8	–0.10	0.20	76
	$EF_{BC}(v_{wind})$	g (kg fuel)$^{-1}$	m s^{-1}	1.4	–0.092	0.30	63
	$CMD(v_{wind})$	nm	m s^{-1}	59	–1.3	0.29	207
	$width(v_{wind})$	nm	m s^{-1}	53	–1.4	0.31	207
atmospheric processes aging	$[NO]/[NO_2](t)$	–	min	0.38	–0.0040	0.19	157
	$[SO_2]/[SO_4^{2-}](t)$	–	min	12	–0.066	0.20	125
	$EF_{NO_x}(JO^1D \cdot t)$	g (kg fuel)$^{-1}$	Hz·s	53	–116	0.13	139
	$EF_{PM_1}(JO^1D \cdot t)$	g (kg fuel)$^{-1}$	Hz·s	6.5	61	0.35	138
	$EF_{SO_4^{2-}}(JO^1D \cdot t)$	g (kg fuel)$^{-1}$	Hz·s	2.8	42	0.45	149
	$EF_{NH_4^+}(JO^1D \cdot t)$	g (kg fuel)$^{-1}$	Hz·s	0.67	20	0.60	76
	$EF_{NO_3^-}(t)$ (main tendency)	g (kg fuel)$^{-1}$	min	0.17	0.0070	0.58	31
	$EF_{organics}(O/C)$	g (kg fuel)$^{-1}$	–	2.3	4.3	0.24	152
	$EF_{PN}(t)$ (night)	# (kg fuel)$^{-1}$	min	$1.5\cdot10^{16}$	$–1.9\cdot10^{14}$	0.36	83
	$EF_{HCHO}(JO^1D \cdot t)$	g (kg fuel)$^{-1}$	Hz·s	0	133	0.89	24
	$EF_{CO}(JO^1D \cdot t)$	g (kg fuel)$^{-1}$	Hz·s	12	189	0.23	111

Table 3: Overview of average quantities of identified ship emission plumes of the AQABA dataset and comparison with plume quantities presented in the literature. The second row contains a brief study description as measurement site / measurement platform / number of investigated ship emission plumes.

		quantity	AQABA 2017	Diesch et al. (2013)	TexAQS 2006 [e]	Jonsson et al. (2011)	Petzold et al. (2008) [h]	Sinha et al. (2003)	Juwono et al. (2013)
			Mediterranean Sea, around Arabian Peninsula / ship / 252	Lower Elbe river bank / mobile laboratory / 139	off the Texan coast / ship / > 200	at Scandinavian harbor / at harbor / 734	English Channel / aircraft / several of same vessel	off the Namibian coast / aircraft / several of 2 vessels	at Australian harbor / on–board / several of 2 vessels
particle phase	EF / g (kg fuel)$^{-1}$	PM	8 ± 2 (PM$_1$)	2.4 ± 1.8 (PM$_1$) [b]	3.32 ± 4.04 (PM$_1$) [b]	2.05 ± 0.11 (PM$_1$)	N/A	N/A	0.7 to 6.1 (PM$_{2.5}$)
		organics	3 ± 1	1.8 ± 1.7	1.26 ± 0.96	N/A	N/A	N/A	N/A
		SO_4^{2-}	4 ± 1	0.54 ± 0.46	1.21 ± 1.50	N/A	N/A	N/A	N/A
		NO_3^-	0.8 ± 0.4	N/A	0.0 ± 0.1	N/A	N/A	N/A	N/A
		NH_4^+	1.3 ± 0.5	N/A	0.0 ± 0.1	N/A	N/A	N/A	N/A
		BC	0.9 ± 0.3	0.15 ± 0.17	0.85 ± 0.76	N/A	0.174 ± 0.043	0.18 ± 0.02	N/A
		PAH	0.011 ± 0.005	0.0053 ± 0.0047	N/A	N/A	N/A	N/A	N/A
		EF$_{PN}$ / # (kg fuel)$^{-1}$	$1.2\cdot10^{16} \pm 3\cdot10^{15}$	$2.55\cdot10^{16} \pm 1.91\cdot10^{16}$	$1.27\cdot10^{16} \pm 0.95\cdot10^{16}$	$2.55\cdot10^{16} \pm 1.1\cdot10^{15}$	$1.36\cdot10^{16} \pm 2.4\cdot10^{15}$	$4.0\cdot10^{16}$ to $6.2\cdot10^{16}$	$1.0\cdot10^{16} \pm 2\cdot10^{15}$ [f]
		CMD / nm	50 ± 10	N/A [c]	N/A	29 ± 3 [f, g]	N/A [i]	N/A	90 ± 10 [f]
		GSD	1.5 ± 0.4	N/A	N/A	1.69 ± 0.04 [f]	N/A [i]	N/A	1.62 ± 0.05 [f]
		width / nm	50 ± 10	N/A	N/A	N/A	N/A [i]	N/A	N/A
		O/C	0.3 ± 0.1	N/A	N/A	N/A	N/A	N/A	N/A
		H/C	1.6 ± 0.8	N/A	N/A	N/A	N/A	N/A	N/A
gas phase	EF / g (kg fuel)$^{-1}$	SO_2	26 ± 6	7.7 ± 6.7	14 ± 12 [f]	N/A	40 to 46	2.9 to 52.2	1.2 ± 0.2 [f]
		O_3	-48 ± 5 [a]	N/A	N/A	N/A	N/A	N/A	N/A
		NO	7 ± 1	16 ± 12	N/A	N/A	N/A	N/A	N/A
		NO_2	35 ± 6	37 ± 20	N/A	N/A	N/A	N/A	N/A
		NO_x (as NO_2)	51 ± 9	62 ± 27 [d]	68 ± 25 [f]	N/A	96 to 109	34.2 to 100.4 [j]	3.4 to 72
		HCHO	1.7 ± 0.8	N/A	0.10 to 0.72	N/A	N/A	N/A	N/A
		CO	20 ± 3	N/A	11 ± 13 [f]	N/A	N/A	3.0 to 19.5	N/A
		[CO_2] / mg m^{-3}	1.0 ± 0.1	N/A	N/A	N/A	N/A	N/A	N/A
		modified combustion efficiency	0.995 ± 0.004	N/A	N/A	N/A	N/A	N/A	N/A
		wt. % fuel S	1.4 ± 0.6	0.38 ± 0.34	N/A	N/A	2.45	0.1 to 2.4	N/A

---

[a] Average reduction of O_3 background level during a ship emission event when considering plume dilution and referring to the amount of burned fuel.

[b] PM EF is given by the sum of EFs of AMS species and of BC.

[c] Count mode is on average (35 ± 15) nm; [g] Value is derived from the average geometric mean diameter and the GSD according to Hinds (1999).

[d] NO_x EF was given as sum of EFs of NO and NO_2 or [j] as NO EF and converted into NO_x EF as NO_2 EF by weighting the NO EF with M_{NO_2}/M_{NO}.

[e] TexAQS: Texas Air Quality Study. Particle phase data are provided by Lack et al. (2009) and gas phase data by Williams et al. (2009).

[f] Average of available data.

[h] Tracking of one single ship emission plume.

[i] Bimodal size distribution observed.

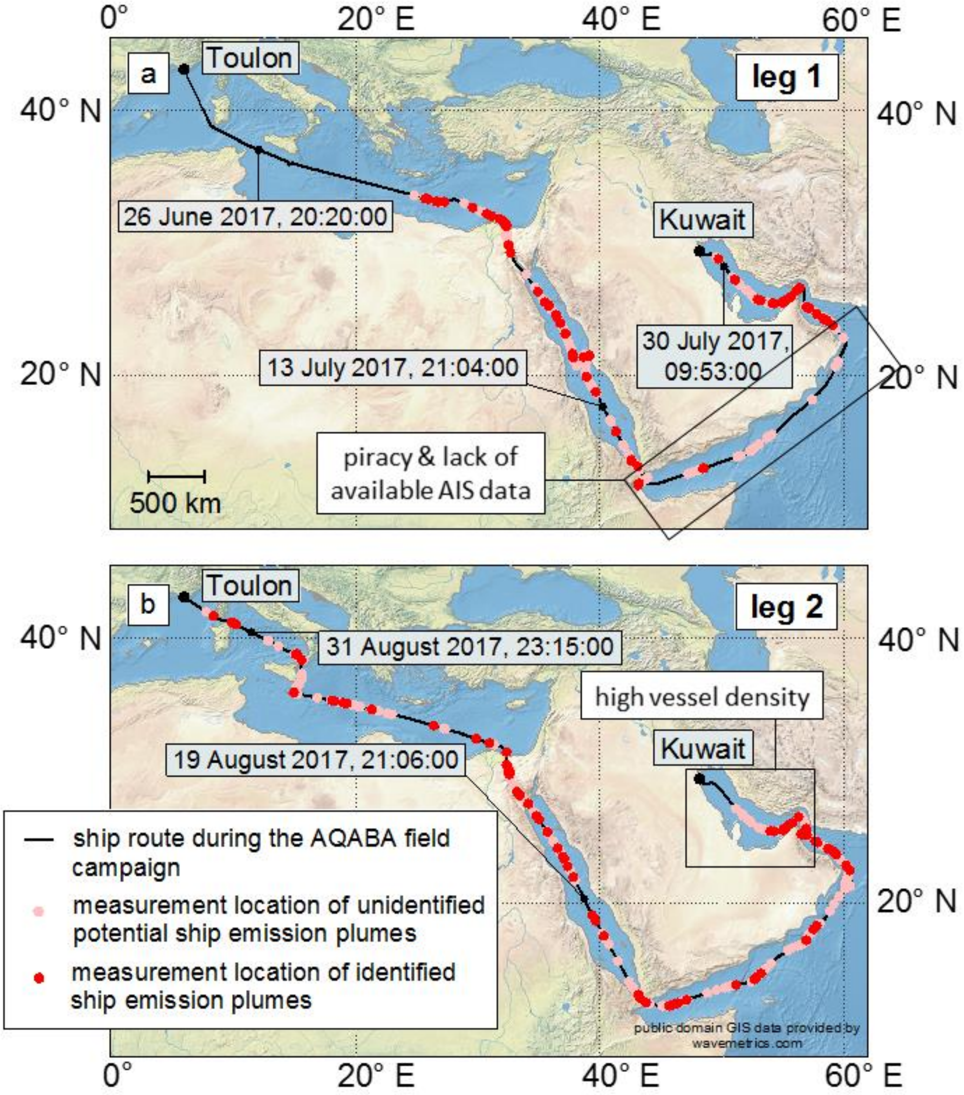

Figure 1: Route of the research vessel *Kommandor Iona* during the AQABA field campaign on leg 1 (a) and 2 (b) with time labels (UTC) for selected geographic positions. The measurement locations of identified and potential, but unidentified ship emission plumes are marked. The Gulf of Aden and the Arabian Sea as well as the Persian Gulf are indicated as areas where the vessel identification was difficult.

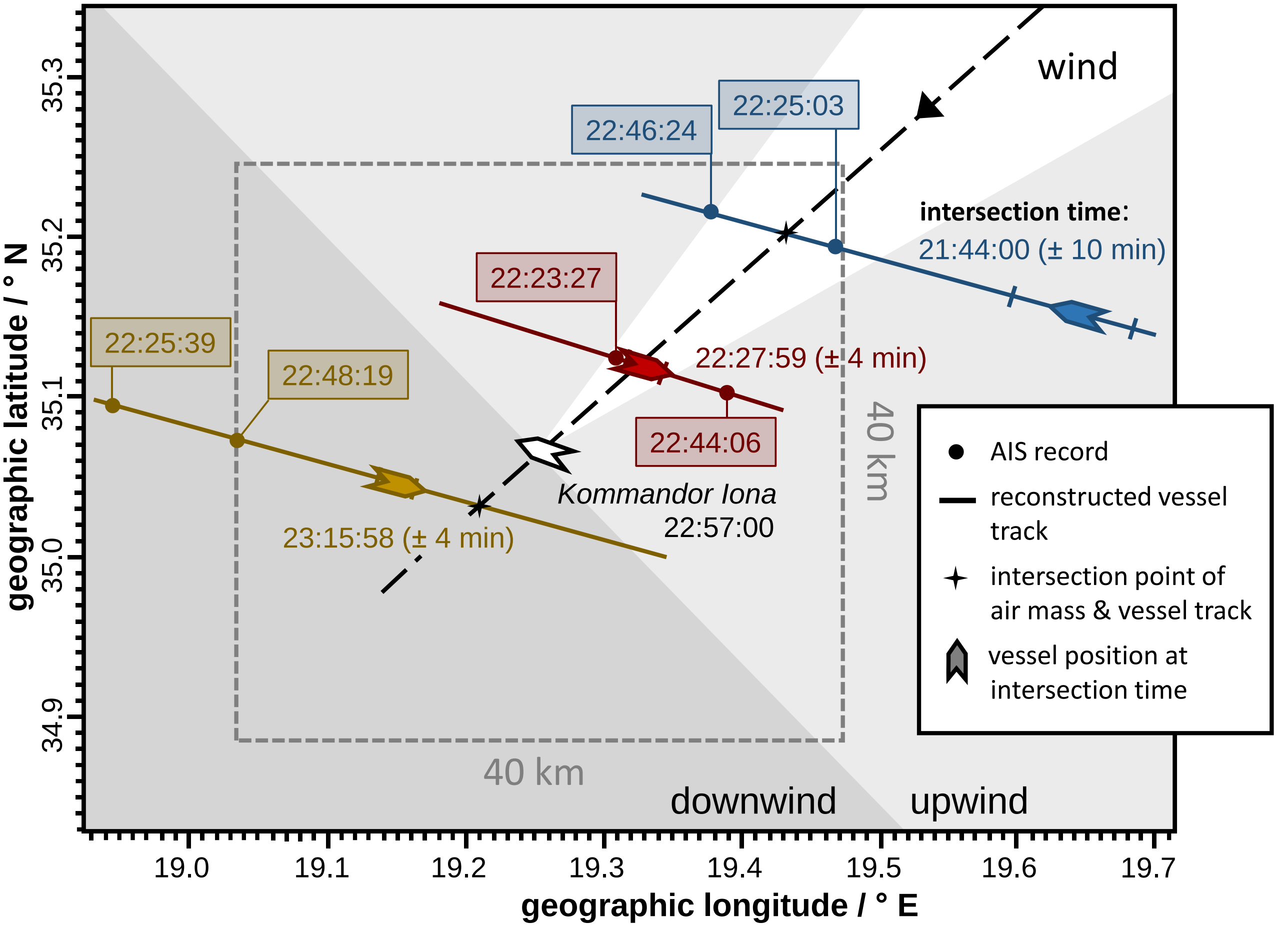

Figure 2: Illustration of the method for the identification of ship emission plumes based on an example event. Vessels to be taken into account had to be in a 40 km × 40 km area around the measurement location during a time interval of 30 min considering the plume measurement time as the interval center. Two AIS records (position indicated by dots on the vessel tracks) were requested after the AQABA field campaign from the AIS data base for each of these vessels, the first one complying with the specified area and time restrictions and the second "previous" one recorded at least 20 min before the first one. Presented are the results of the calculations based on the measurement time and location, the average wind data, their uncertainties and the available AIS records. The areas down– (dark gray) and upwind (light gray) of the measurement location refer to the average wind direction (dashed line; uncertainty is indicated by the white area). The uncertainties of the intersection times and of the corresponding vessel positions (ship markers on the vessel tracks) are based on the uncertainties of the wind speed. In this specific case, the vessel *Cape Flamingo* (red) was identified as emission source.

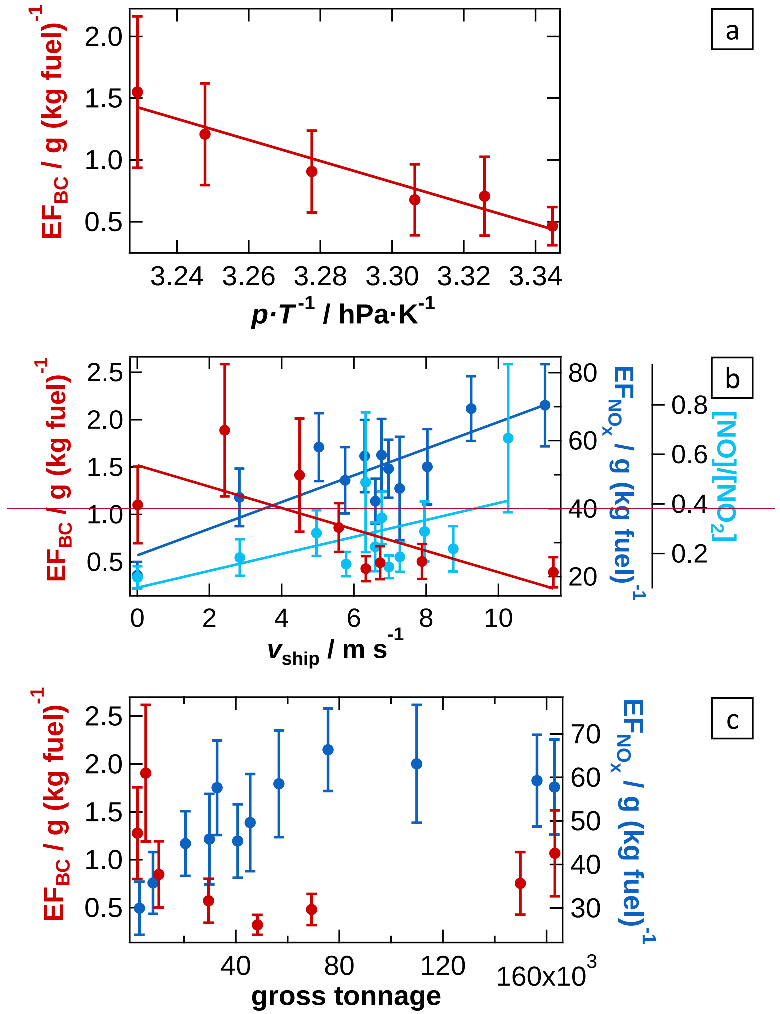
a
EF$_{BC}$ / g (kg fuel)$^{-1}$
2.0
1.5
1.0
0.5
3.24
3.26
3.28
3.30
3.32
3.34
$p \cdot T^{-1}$ / hPa·K^{-1}
b
EF$_{BC}$ / g (kg fuel)$^{-1}$
2.5
2.0
1.5
1.0
0.5
0
2
4
6
8
10
v_{ship} / m s^{-1}
80
60
40
20
EF$_{NO_x}$ / g (kg fuel)$^{-1}$
0.8
0.6
0.4
0.2
[NO]/[NO$_2$]
c
EF$_{BC}$ / g (kg fuel)$^{-1}$
2.5
2.0
1.5
1.0
0.5
40
80
120
160x10^3
gross tonnage
70
60
50
40
30
EF$_{NO_x}$ / g (kg fuel)$^{-1}$

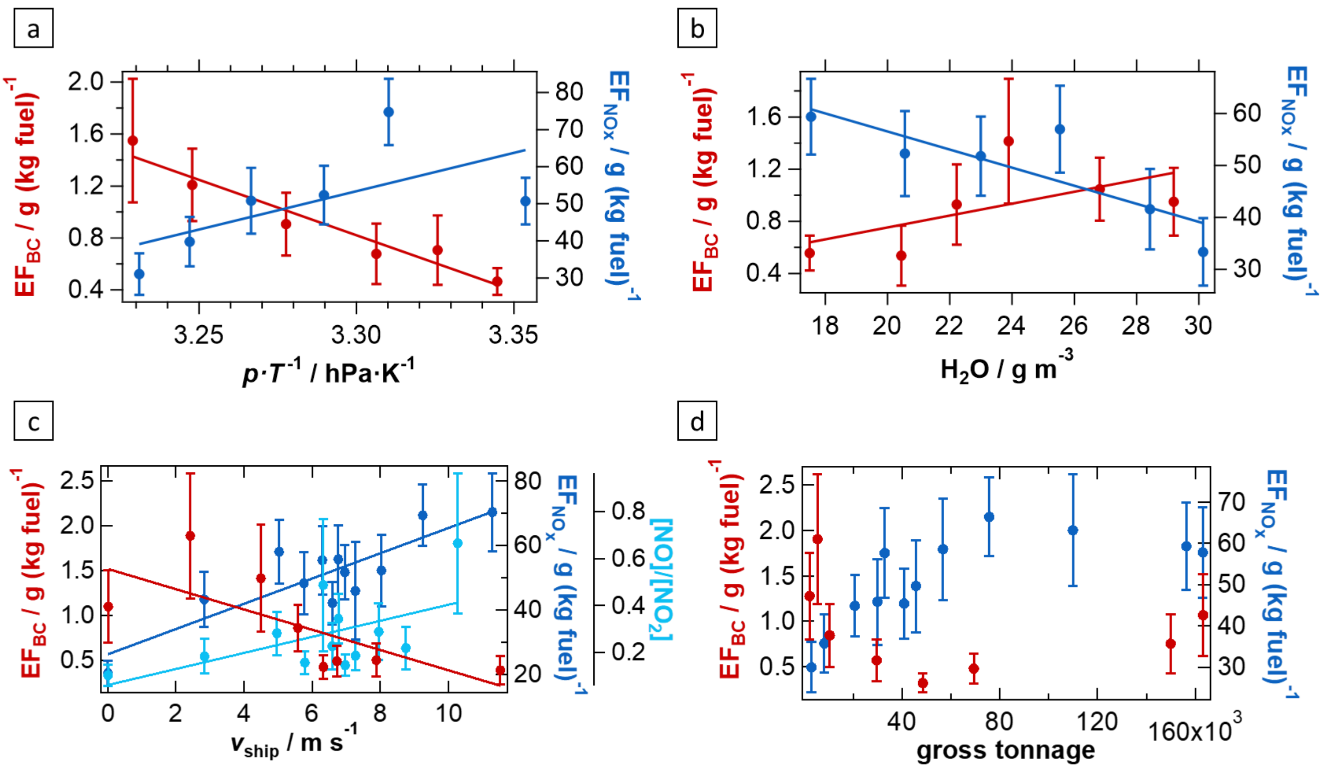

Figure 3: Influences of combustion conditions on ship emission plumes. The dependencies~~y~~ of the NO_x and BC emission factors on the ratio between atmospheric pressure and ambient temperature (a) and on ambient water vapour concentration (b) are~~is~~ demonstrated~~ (a)~~. Additionally, the dependencies of the NO_x and BC emission factors as well as of the NO to NO_2 ratio of average excess concentrations on the vessel speed are presented (~~b~~c). The correlations between the NO_x and BC emission factors and the vessel gross tonnage are shown (~~c~~d). Error bars present the combination of estimated quantification and measurement uncertainties and one sigma standard deviations of the data distributions in each bin. The corresponding fit parameters and correlation coefficients are listed in Table 2.

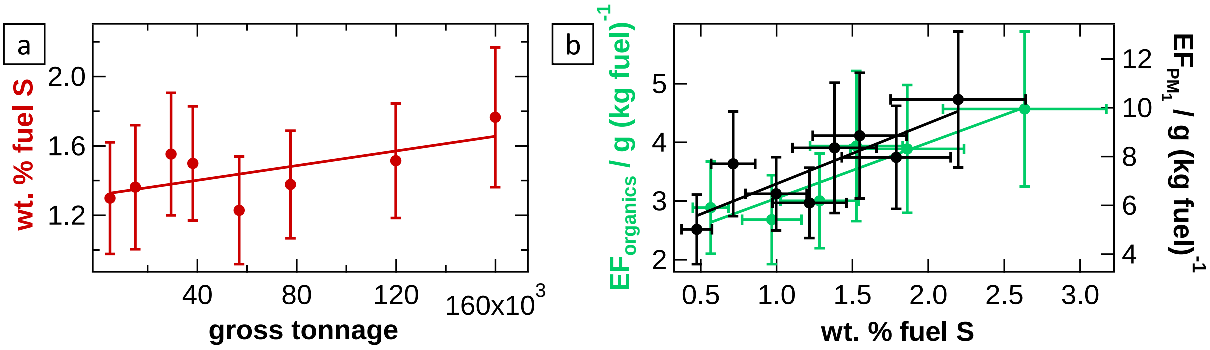

Figure 4: Influences of fuel quality on ship emission plumes. The correlation between the weight percentage of fuel sulfur and the ships' gross tonnage (a) and the dependencies of the particulate organic as well as the PM_1 emission factors on the weight percentage of fuel sulfur (b) are shown. The fit parameters and correlation coefficients are listed in Table 2.

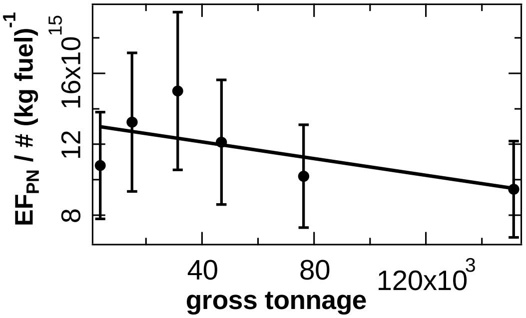

Figure 5: Influence of the exhaust system's size (in terms of gross tonnage) on ship emission plumes. The particle number EF is plotted versus the gross tonnage of the ship. The fit parameters and correlation coefficient are listed in Table 2.

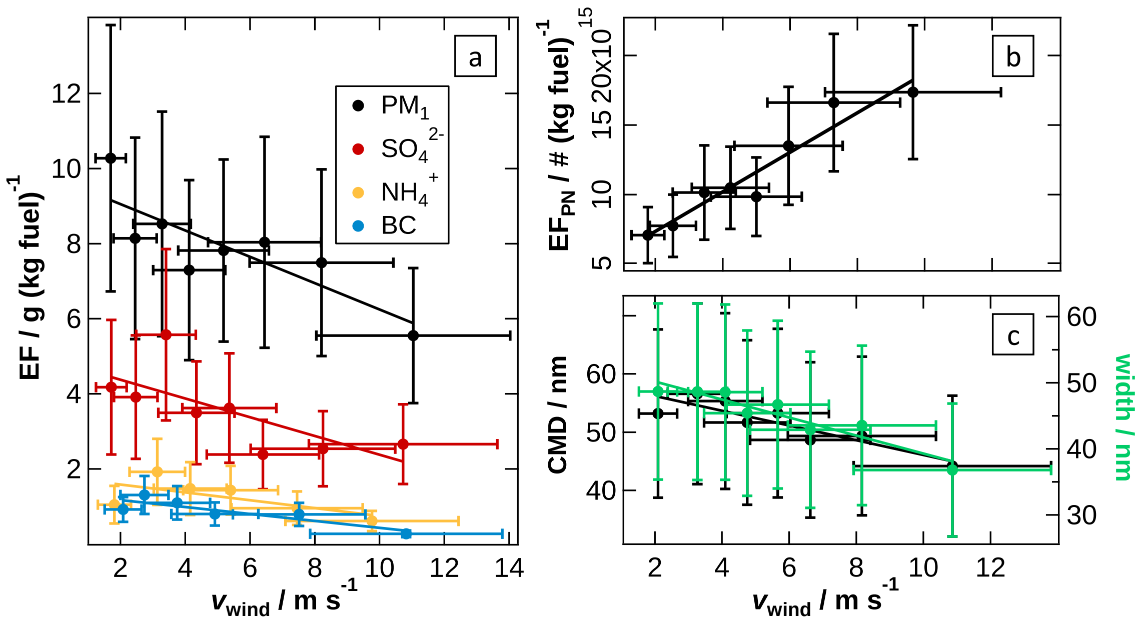

Figure 6: Effect of dilution during the early stage of plume release on ship emission plumes. PM_1, SO_4^{2-}, NH_4^+, BC (a) and particle number emission factors (b) as well as the CMD and width of the particle number size distribution (c) are plotted versus the wind speed. The fit parameters and correlation coefficients are listed in Table 2.

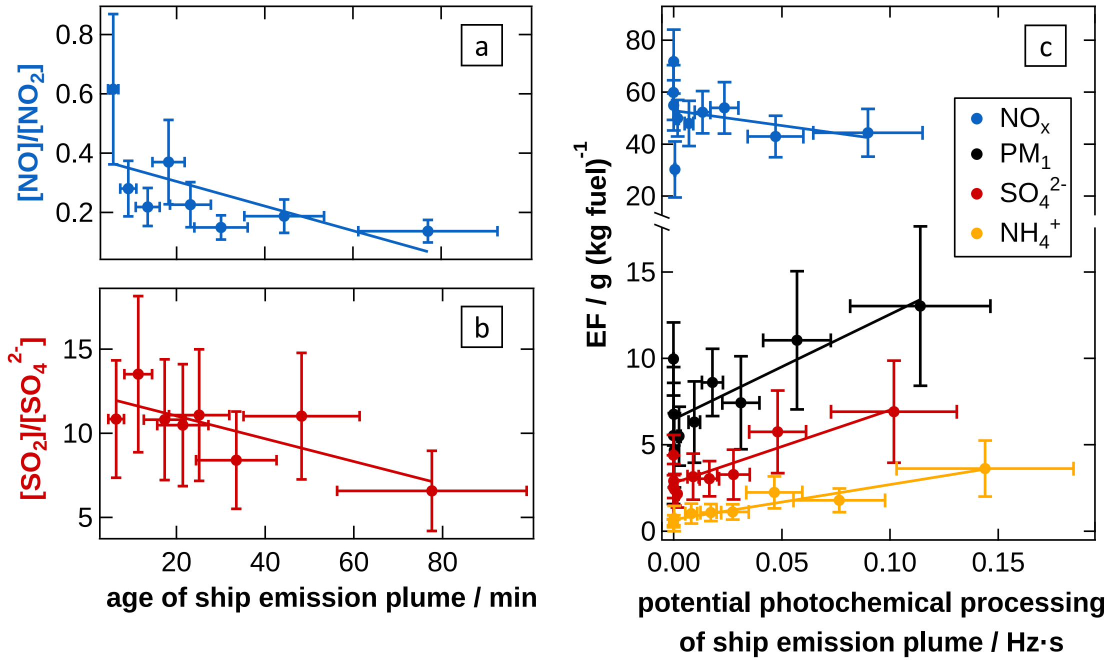

Figure 7: Atmospheric processing of nitrogen and sulfur species in ship emission plumes. The conversion of NO into NO_2 (a) as well as the conversion of SO_2 into SO_4^{2-} (b) during plume aging are demonstrated through the development of the average excess concentration ratios. Additionally, the decrease of NO_x and increase of PM_1, SO_4^{2-} and NH_4^+ with increasing potential photochemical processing of ship emission plumes (measured/calculated JO^{1}D integrated over the plume transport time) are shown using the development of the apparent emission factors as indicator (c). The fit parameters and correlation coefficients are listed in Table 2.

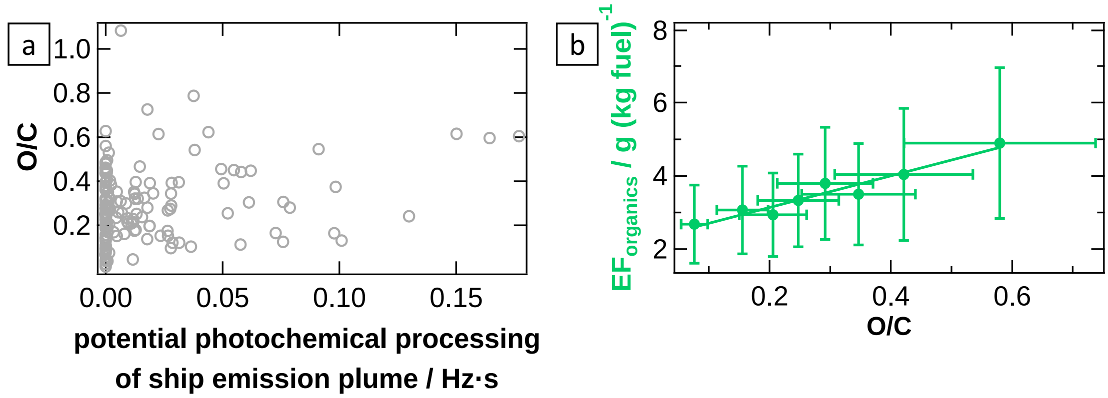

Figure 8: Development of particulate organics and their oxidation level during atmospheric aging of ship emission plumes. The correlation between the O/C ratio (rel. uncertainty (combined rel. quantification and measurement uncertainties): 48 %) and the potential photochemical plume processing (avg. rel. uncertainty: 27 %; measured/calculated JO^{1}D integrated over the plume transport time) (a) as well as the correlation between the apparent emission factor of particulate organics and the O/C ratio (b) are shown. The fit parameters and correlation coefficient are listed in Table 2.

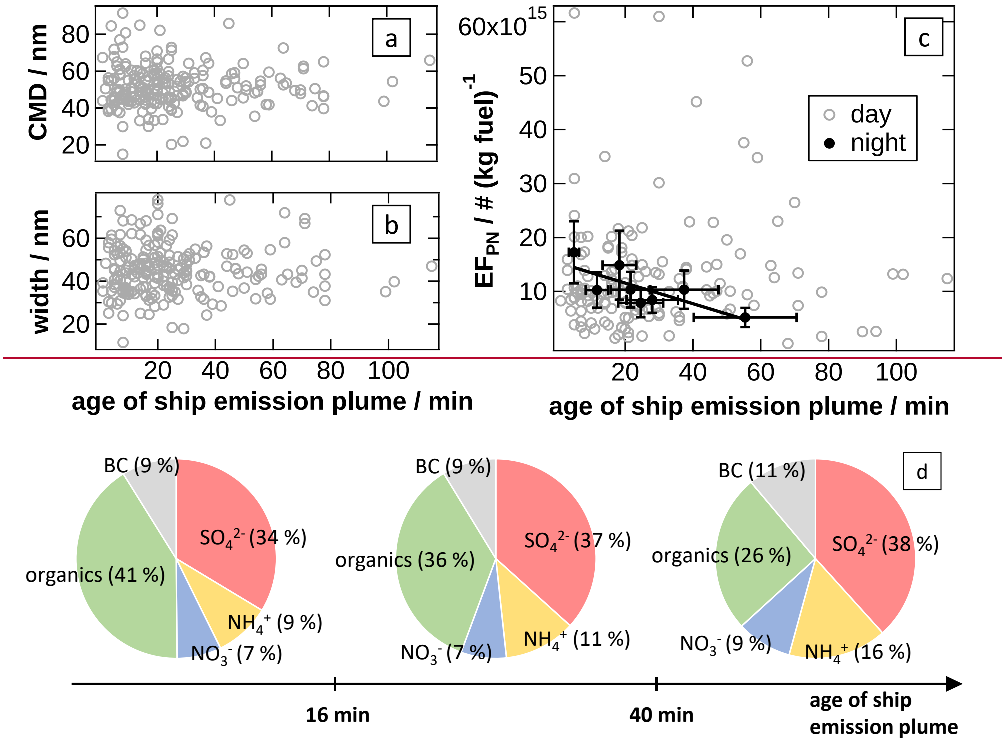
a
b
c
d
CMD / nm
width / nm
EF_PN / # (kg fuel)^-1
60x10^15
day
night
age of ship emission plume / min
age of ship emission plume / min
BC (9 %)
SO4 2- (34 %)
organics (41 %)
NH4 + (9 %)
NO3 - (7 %)
BC (9 %)
SO4 2- (37 %)
organics (36 %)
NH4 + (11 %)
NO3 - (7 %)
BC (11 %)
SO4 2- (38 %)
organics (26 %)
NO3 - (9 %)
NH4 + (16 %)
16 min
40 min
age of ship emission plume

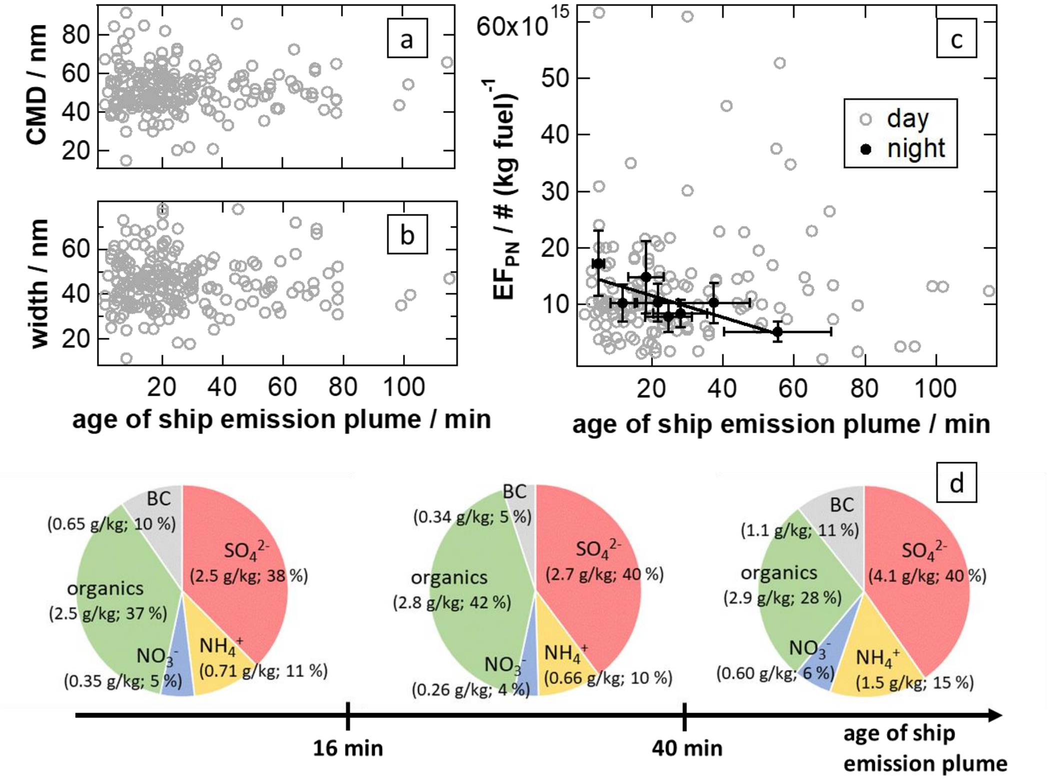

Figure 9: Influences of atmospheric processing on the particle phase characteristics of ship emission plumes. The CMD (rel. uncertainty: 27 %) (a) and width (rel. uncertainty: 27 %) (b) of the particle number size distribution and the apparent particle number emission factor (rel. uncertainty: 26 %) (c) are plotted against the age of the ship emission plume (avg. rel. uncertainty: 20 %). The fit parameters and correlation coefficient are listed in Table 2. Additionally, the ~~average~~ typical chemical composition (calculated from median EFs) of the particle phase is given for ship emission plumes younger than 16 min, between 16 and 40 min of age and older than 40 min (d).

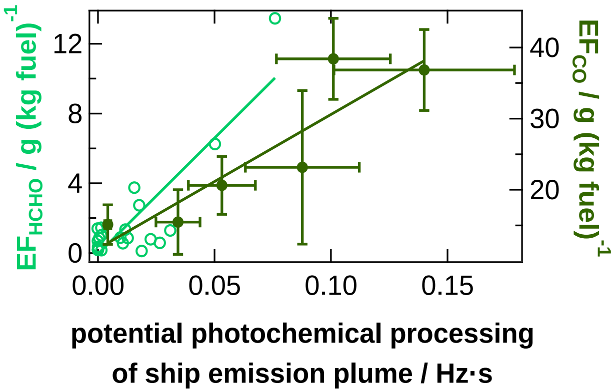

Figure 10: Influence of atmospheric processing on HCHO (rel. uncertainty: 29 %) and CO in ship emission plumes observed during AQABA. For both cases, the development of the apparent emission factor with increasing potential photochemical plume processing (avg. rel. uncertainty: 27 %; measured/calculated $J\mathrm{O}^1\mathrm{D}$ integrated over the plume transport time) is presented. The fit parameters and correlation coefficients are listed in Table 2.

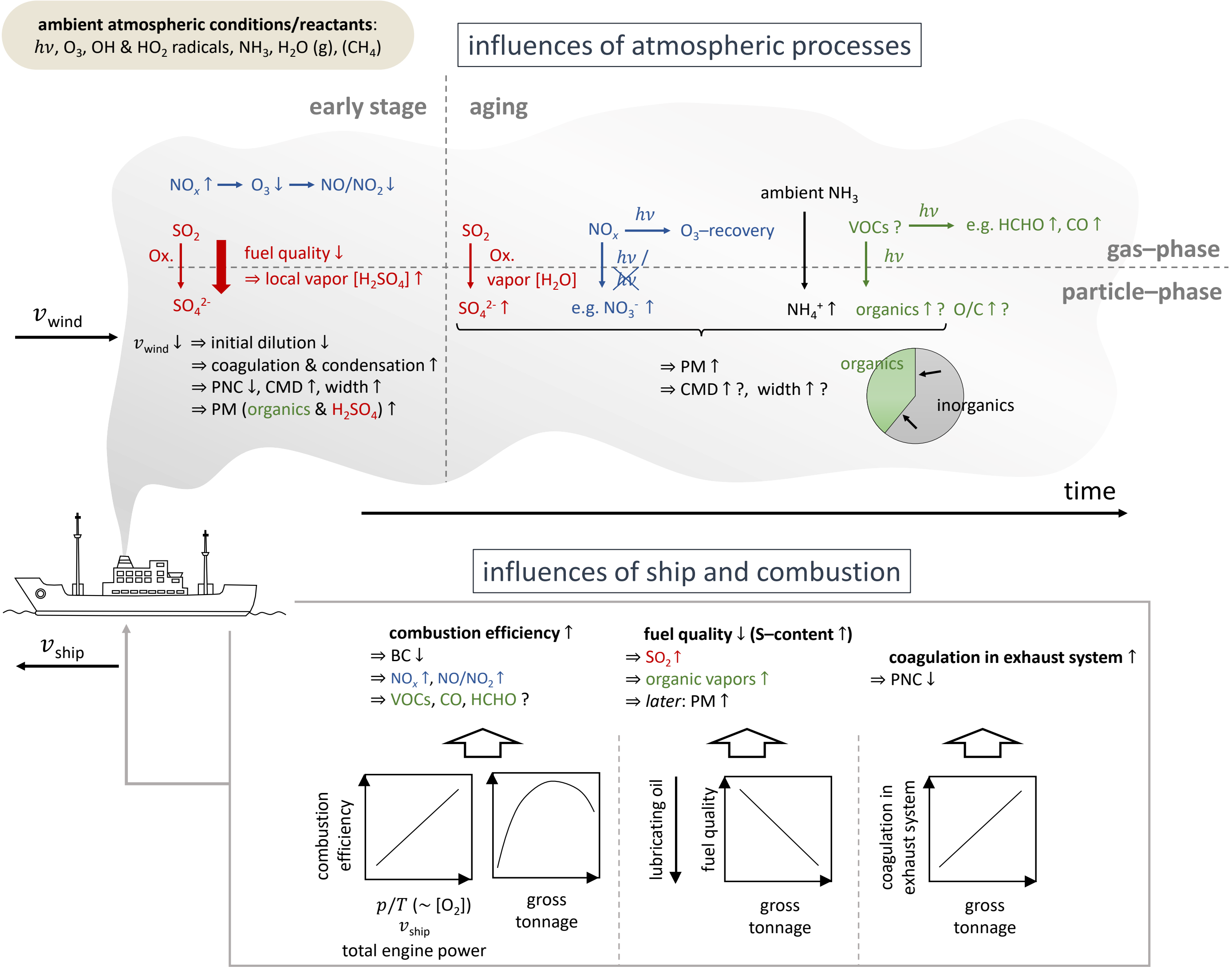

Figure 11: Qualitative overview of the observed dependencies of ship plume characteristics on ship parameters and conditions during the combustion process as well as on atmospheric processing immediately after plume release and during plume aging.